Application Note

A Practical Guide of Deconvolution

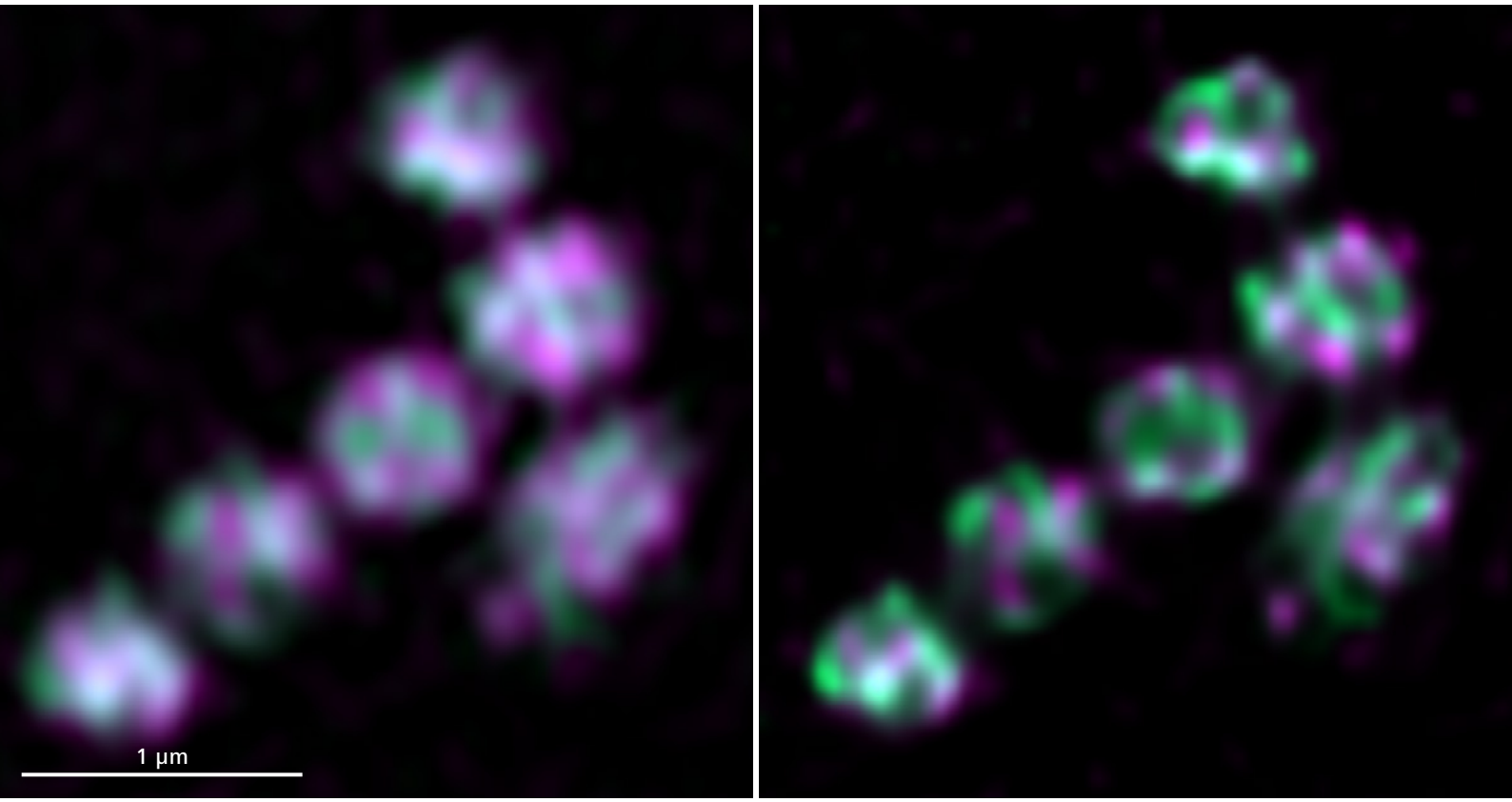

Seeing beyond

Contents

Cover image:
Mitochondria in an *Arabidopsis thaliana* cell. mCherry (green) is targeted to the matrix and GFP (magenta) to the intermembrane space. Comparing Airyscan SR (left) and Airyscan Joint Deconvolution (right). Courtesy of J.-O. Niemeier, AG Schwarzländer, WWU Münster, Germany

Authors: Olivia Prazeres da Costa, Ralf Engelmann, Martin Gleisner, Lutz Schäfer, Xianke Shi,
Eva Simbürger, Max Voll, Klaus Weisshart, Georg Wieser
Carl Zeiss Microscopy GmbH, Germany
Date: December 2021

Introduction

Since the introduction to widefield fluorescence microscopy in 1983, deconvolution has witnessed the development of a wide variety of algorithms. It has been successfully and routinely applied to almost all microscopy techniques. There has been especially a sharp rise in the popularity of deconvolution for the past decade, mainly fueled by the rapid improvement of computer hardware, particularly by the advance of NVIDIA® CUDA® technology and the parallel processing power of graphic processing units (GPUs). The speed of deconvolution, which used to be the bottleneck of the method, has been dramatically improved, e.g., up to 30x faster with a modern GPU compared to traditional central processing units (CPUs). Due to these advantages in computer hardware, deconvolution has left its somewhat dated state and has experienced an impressive revival. It is now an integral part of many microscopy applications.

For widefield microscopy, deconvolution is the method of choice to improve image quality. The algorithm reassigns the out-of-focus blur in the 3D stack, the primary source of noise in widefield microscopy, back to the in-focus plane as the signal. The result is better contrast, higher signal-to-noise ratio (SNR) of the in-focus structures, and increased resolution. The on-the-fly implementation of deconvolution for widefield fluorescence microscopy thus provides a gentle and fast 3D capability, highly suitable for cell biology and bacteriology application. In recent years, images from laser scanning confocal and spinning disk confocal microscopes have also been regularly processed with deconvolution. Using mainly iterative-based algorithms, coupled with scanning oversampling and reduced pinhole size, confocal deconvolution has been proven to increase lateral and axial resolution beyond the theoretical diffraction limit. At the expense of speed and sensitivity, confocal deconvolution has become the most affordable super-resolution (SR) technique. The most recent advances in deconvolution are in the traditional hardware-based SR microscopes: Structured Illumination Microscopy (SIM) and Image Scanning Microscopy (ISM such as ZEISS Airyscan). Both SIM and ISM require dedicated multi-phase raw data acquisitions. The subsequent reconstruction process usually involves a linear inverse filter-based deconvolution, most noticeably a Wiener Filter. However, by carefully implementing an iterative-based algorithm and a dedicated point spread function (PSF) model, it is possible to drive the resolution down to the sub-100 nm domain, opening new possibilities for SR live-cell imaging. This has been successfully demonstrated by the dual iterative SIM process of ZEISS Lattice SIM, and the Joint Deconvolution process of ZEISS Airyscan 2.

This white paper aims to provide a practical guide for users of deconvolution in an easy-to-understand language and with minimum specialized terms. It will address three main questions: what is deconvolution? Why should I use deconvolution for my microscopic images? How do I use it correctly?

What is Deconvolution?

Generally speaking, deconvolution is a mathematical method used to reverse the unavoidable impact of optics and electronics. Deconvolution has different areas of application such as seismology and astronomy as well as microscopy. The reversal has shown to improve resolution, contrast and signal to noise ratio (SNR).

The point spread function (PSF) is used to describe the blurring of the sample seen in the resulting image. In widefield microscopy for example, the PSF has a double cone-like shape that extends infinitely into axial direction

Photon assignment and reassignment, what does this mean?

Assignment (forward model)

The picture of a sample seen through a microscope often appears blurry. This is due the fact that optics merge (by adding) information from locations other than specific points of interest in the sample. Thereby, the size and form of the spread from these locations is known as PSF. In contrast, what the microscope does is often called super-position or convolution.

Reassignment (reversing the forward model)

The idea to reverse the microscopes blurring is obvious. It would require subtracting intensities where they have been wrongly added, but also adding intensities to locations where they were taken from. Overall, in this process called deconvolution, the sum of all intensities remains the same before and after the procedure. Therefore, conservation of energy is preserved, and quantitative measurements can be conducted.

Reassignment problems

Unfortunately, deconvolution is not free of uncertainties in both location and intensity of the reassignment. These uncertainties originate from errors in the intensity measurement and the PSF. The mathematical term, where such errors alter the result of reassignment is called *ill-posed problem*.

Deconvolution wants to pick intensities from the observed image and re-assign them, by convolving the inverse of the PSF. Due to lacking precision, sparse data, noise and other factors (such as the infinite extension of the PSF in the wide field case) the deconvolution becomes an ill-posed problem, meaning that there is no single solution. This is the reason why different algorithms have been implemented.

The solution space also encompasses undesired solutions, such as negative intensities causing oscillatory artifacts and other problems. Since the early 1970's exists a large body of publications that deal with such problems from a rigorous mathematical point of view. Today, it is well understood that eliminating undesirable solutions is the key to artifact free, successful reconstructions. The solutions are implemented and available in the ZEISS deconvolution framework.

Algorithms implemented in ZEISS ZEN (blue edition)

Deblurring

Deblurring attempts to subtract contributions from approximated out-of-focus information. The main advantage is that it speeds up computation and thus allows this method to be part of data acquisition. Deblurring is also known as no neighbor or sometimes as unsharp masking. By virtue, this method cannot reconstruct quantitatively correct results.

Nearest Neighbor (NN)

NN was the first pragmatic attempt (Castleman 1975) to de-blur 3D microscopic data with a 2D method similar to deblurring. Due to computational limitations of the time, rigorous mathematical treatment was not an option. Therefore, only a simplified additive model was considered in which approximated out-of-focus contributions that were subtracted from in-focus information. It does not consider a true 3D inversion as today's rigorous methods. Instead, it uses 2D planes with the side effect of being insensitive to axial sampling. This allows to successfully use image data that does not adhere to Nyquist sampling restrictions. Otherwise, by design this algorithm will not provide quantitatively correct results.

Regularized Inverse Filter (RIF)

RIF (or linear least squares) uses a direct, linear inversion of the forward model. It can also be seen as a standard convolutional filter using an inverted PSF. To counter instability due to ill-posedness (e.g., noise and PSF singularities) regularization is added (Tikhonov and Arsenin 1977), also known as Wiener Filter (Wiener 1949).

Fast Iterative (Meinel/Gold's method)

Around the beginning of the 1970's a new, iterative approach was introduced to one dimensional restoration of spectral data. There, the forward problem is applied to a guess-image that can be chosen more or less of the expected result at the beginning of the algorithm. The result of this is then compared to the observed image and the residual is applied to correct the guess. This process is repeated until the correcting residual has vanished to very small values. Such algorithms can be implemented where the said residual is computed as a difference (Jansson 1996, van Cittert 1931) or as a ratio (Meinel 1986). Due to the possibility to impose corrective modifications with every guess, these types of algorithms are also known as constrained iterative. The most popular constraint is positivity. In the case of Meinel (which is available in the ZEISS framework), positivity is implicit. This algorithm requires only a few (less than 10) iterations to complete and is therefore quite fast. However, there is a caveat: this method only works correctly on perfectly symmetric PSFs which, unfortunately, are rarely present when immersion oil is the primary source for aberrations not known to the system.

Fast Iterative: Richardson–Lucy classical iterative

To overcome the disadvantage of the Meinel algorithm, which only works on perfectly symmetric PSFs, a rigorous statistical approach such as maximum likelihood is required (Richardson 1972, Lucy 1974). The maximal likelihood of the sample is determined by the given observation and its parameters (e.g., PSF). Surprisingly, this leads to a simple extension of the Meinel algorithm. The only downside is that many iterations (sometimes thousands) are required. Also, another caveat is that with a rising number of iterations, the result becomes instable, and the likelihood will decrease again at some point.

Fast Iterative: Accelerated Richardson–Lucy

To reduce the high number of iterations, a somewhat heuristic gradient-based acceleration scheme has been developed and shows promise for success (Biggs 1986). This algorithm essentially converges to almost the same result as the Richardson–Lucy algorithm but in about an order of magnitude fewer iterations.

Constrained Iterative: MLE

Given the promising results of the accelerated Richardson–Lucy algorithm, there is still the possibility for instability during very high numbers of iterations due to missing regularization. Additionally, the acceleration based on linear gradients may not lead to robustly converged results.

Faster convergence (fewer iterations) combined with variable choices for the types of likelihood and regularization can be obtained by a generalized conjugate gradient maximum likelihood algorithm (Schaefer et al 2001). This is the current ZEISS standard for high performance deconvolution.

Combined (joint) Deconvolution

It is well understood that more and diversely collected information around the sample can reveal greater detail and therefore higher resolution than single view observations. Today, in the era of SIM, ISM, LFM and SPIM, several instruments appeared on the market that would take multiple views of one sample with the expectation being to reveal more information. While each of these methods focuses on different physical properties of illumination and observation angles, the resulting images always have at least one or more added raw data dimensions. With respect to the sample, this offers not only the possibility of reconstruction, but also including their respective PSFs in this process. An algorithm that can fuse and reassign all collected spatial content into one single reconstruction, called joint deconvolution, is superior to previously known methods. It can be shown that the various viewing angles of the sample result in a larger optical-transfer function (OTF) support, in addition to the observed detail out of every view. Therefore, an exceptional increase in resolution to and below 100 nm can be expected and has been shown with the Airyscan joint iterative deconvolution recently released by ZEISS.

What is the point spread function (PSF)?

The PSF describes the measure of blur in a given imaging system. An optimal PSF is key to improving the quality of the image as a result of the deconvolution. Kinds of PSFs:

Measured

Measuring a PSF is done by acquiring an image of sub-resolution sized fluorescent beads, typically 100 nm in diameter. By using a software wizard, the user can select the beads from a batch that are spaced sufficiently away from each other and are in decent condition. The selected beads will then be registered automatically and averaged to form the final space invariant PSF.

How to generate a measured PSF?

Using a measured PSF can potentially improve the deconvolution result, especially with data acquired using high NA objectives (NA>1.2). PSF measurement is also an excellent approach to evaluate the current optical condition of your microscopes and should be carried out regularly. However, the procedure is daunting to most first-time users, and it requires proper preparation and practice. View a brief guide on how to generate a measured PSF *here*.

Theoretical

It is faster and easier to compute a PSF than to use the physical instrument PSF. Here we can choose between scalar and vectorial PSF models. The vectorial PSF is usually more precise and allows for polarized illumination light (Born, M. & Wolf, E. 1959). Most PSF models in the ZEISS deconvolution system can be adjusted for spherical aberration (Gibson, S. & Lanni, F. 1992) caused by layers of varying refractive index due to mounting of the sample. These layers consist of immersion, coverslip and embedding material.

Depth variant (theoretical)

Furthermore, a PSF can be computed to be variable over the sample depth in the form of multiple PSFs for each chosen depth. In this case most processing methods will operate in depth variant mode, reconstructing spatial features along the optical axis until the image is significantly improved.

ZEN PSF standard:

The ZEN CZI format of a PSF has been standardized for all available microscopes manufactured by ZEISS and others.
It will work with all deconvolution functionalities, despite their possibly different options.

Why do we have optical distortion?

Noise, scatter, glare, blur (see also Wallace 2001)

Noise originates from:

1) Fluorescence generation and Poisson distribution of emission as a function of observation
2) Electronic noise, thermal noise, readout noise and discretization noise (mostly additive Gaussian distributions in the observation)

Both sources are covered by the imaging model.

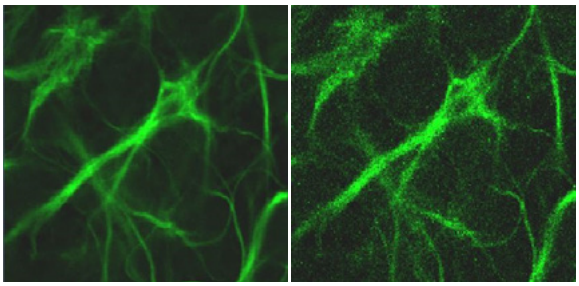

Figure 1 *Murine brain Astrocytes labeled for GFAP (Alexa 488). Comparison of a slow (left) and a fast (right) scan on an LSM 800.*

- **Scatter**
  Caused by light passing through turbid media within the sample. Due to complicated modelling this is currently not considered.

- **Absorption**
  Caused by light passing through absorbing, dense media within the sample. Due to nonlinearity, it is not considered in the imaging model.

- **Glare**
  Caused by internal reflections of bright sources of light in low light areas. This cannot be considered in the imaging model.

- **Blur**
  Caused by the impact of the PSF. This is fully covered in the imaging model.

Practical Guide

General recommendations

What are the general recommendations for image acquisition settings if the resulting images are meant to be processed with a deconvolution algorithm?

The key to best results for deconvolution is to present an optimal input image to the algorithm. And the optimal image is the one with the highest possible signal and the lowest possible noise. In addition, the sampling rate, which in a confocal system then determines the number of pixels in the resulting image, must be high enough. What is high enough? The sampling rate must result in an image where the size of each pixel is less than half of the size of the structure you want to resolve, provided that the system supports this sampling. The theorem of such a sampling is called Nyquist–Shannon criterion for sampling. This means, you need to know the resolution of the optical system to get the sampling right – especially if the sampling can be changed, like on a confocal system. Typically, your confocal system provides information on the current sampling rate for a given acquisition setting. The sampling can then be changed to comply with Nyquist or even go beyond (like 2 × Nyquist for Airyscan, as detailed below). When the acquisition is performed with a camera, the optical system is designed to comply with Nyquist and settings don't have to be changed. However, you need to be careful when you increase the size of the pixels by binning. This method then requires special consideration, and you must know the resolution of your system to be able to predict potential consequences.

How do you generate such an image from your specimen?

For widefield systems, the camera has a set number of pixels which is typically high enough to process the resulting images with deconvolution. For confocal systems, the sampling needs to be defined for the current optical parameters which include the objective, zoom and detection range apart from the size of the pinhole. Modern user interfaces do provide some way to set the sampling to the necessary rate to match the Nyquist criterion.

Once the sampling is set the acquisition parameters need to be balanced to achieve a bright signal with low noise. With camera images this means optimizing exposure time to get a bright image. However, the brightness should not exceed the value of 50% of the total dynamic range. This can be checked when looking at the histogram, a graph to display the distribution of the signal intensities over the given grey scale. If the intensities are mainly located in the range up to 50% of the grey scale, the settings are good to go – for imaging one sample plane. For confocal systems, this prerequisite is less of an issue because the applied algorithms take care of this. In any case saturating the image absolutely must be avoided; no pixel should be at or over the maximum grey level. Check with a range indicator that shows saturated pixels in an obvious color scheme.

For confocal acquisition, there are additional ways to optimize the signal to noise ratio. One way is to increase excitation light and lower the detector gain, but this might result in phototoxic effects like bleaching, which are unwanted effects since bleaching again reduces the signal, but only to a smaller extent reduces the noise. To find a good balance, one trick is to mimic the acquisition, first without laser light, then increase the detector gain to the limit where electronic noise is not yet visible. Other strategies do not change laser settings but rather

change the illumination time per pixel by decreasing imaging speed or by averaging the signal over 2 or more scans. But again, this increases the light dose onto the sample.

Typically, you want to look at three-dimensional structures, whether you use a camera for imaging, maybe even paired with structured illumination, or you use a confocal system. The Nyquist–Shannon theorem, our sampling prerequisite, also applies to the third dimension. The required number of images in Z is again defined by the point's emission signal as specified by the PSF. However, for any deconvolution algorithm to work with 3D data, you need to acquire enough "dense" images in Z as well as enough images. Typically, the software provides some indications for how to choose the right sampling in Z. To determine the range of images required in Z, you need to know the attainable resolution of your system. If you know the extension of the PSF in Z, the imaged Z-range should cover at least 3 – 5 times the size of the PSF. When using a confocal system, the sampling rate is dependent on the slice thickness indicated in the user interface, with the optimal settings suggested. The total range is dependent on what you want to see in Z but a minimum of 5 slices is required for the DCV to work. Now that you have optimized the settings, you will figure out that this does have some consequences to the overall imaging process.

First and immediately observed, image acquisition takes longer. The higher number of pixels in XY and the higher number of images in Z both increase acquisition time compared to other settings in which you don't consider these parameters. Imaging for the purpose of applying deconvolution can be time consuming especially using laser scanning confocal microscopes – but most often it's worth it! However, longer acquisition time means longer excitation time, which means greater risk of bleaching the sample.

How can you deal with this drawback?

The most effective thing to do is to choose as small an area as possible for imaging to reduce the field of view to the required size only. High resolution or super-resolution is typically applied to already tiny, subcellular structures, so restricting the scanned area to the structures of interest reduces the frame size and therefore the imaging time for each frame. This not only helps to speed image acquisition but also speeds the subsequent data processing. For a widefield system this might not be so relevant, however, if binning of pixels still provides a high enough sampling rate, at least data processing will be faster. The amount of data the algorithm must process determines the amount of time it takes to get the result.

If the highest resolution is not the most important aspect to be achieved with DCV but rather the reduction of noise and some deblurring, then using a lower sampling rate might be a good option. It helps to speed image acquisition and reduces the light impact onto the sample. This approach will still produce high quality images with better visible structures, although they are not maximally resolved.

What about a moving target?

Whenever you have a fixed sample and nothing is moving, then the point of origination for the emission signal is known. Whenever you have a living sample like cultured cells, organoids, or whole organisms of various size, the structure you want to look at may be in motion while you acquire a single image or an image stack series. Depending on the speed of this movement, the application of deconvolution to those images may be impossible, not only with scanning systems where line by line the point of interest might move but also with camera images. Even a short exposure time can result in a blurred image. If you cannot shorten imaging time, then try to slow down potential movement of the sample. Knowing the sample and its potential for movement is crucial in this case.

If imaging requires a specific duration, how can you speed the time-to-result?

The total amount of data needed determines the total processing time. The aforementioned measures of modern programming using graphical processors brought the time-to-result to a range where it became way more attractive to use deconvolution algorithms in the first place. A very good approach to processing large data sets is to do it during image acquisition. System set-ups with additional processing computers are offered, with an automatic transfer of data to start the processing whenever enough data have arrived. You will then see the result shortly after the experiment has finished.

Anything else to consider? A word on the objective lens

The objective you choose is the first interaction with the sample. Any damage to the objective will result in bad images from the start, no matter how you take care of the rest of the set-up. Keep it clean. Chose an objective where the refractive index of the immersion medium matches the index of the embedding medium. Higher numerical aperture (NA) of the objective will not solve the problem of getting higher resolution unless these indices are correct. Change the embedding medium if needed – you will see the result immediately. For a detailed discussion on cleaning microscopes, please refer to ZEISS "The Clean Microscope" brochure.

Deconvolution methods

The classical deconvolution for fluorescence widefield microscopy

Fluorescence microscopy has significantly advanced life science research. In the past century, many major discoveries in cell biology and neuroscience were possible only because of direct visualization of cells, subcellular components, and their mobility and interaction with others. Fluorescence microscopy plays a pivotal role in such direct visualization. By labelling specific molecules or structures with a light-emitting fluorophore, small particles and delicate structures can be identified and quantified with much higher specificity and precision. Fluorescence microscopy was pioneered by ZEISS at the beginning of the twentieth century. Fast forward to today and it remains one of the most widely used instruments in any biology research lab.

Traditional fluorescence widefield microscope has a straightforward yet elegant epi-illumination beam path design. The essential feature is to provide a mechanism to illuminate the sample with a selected wavelength range, then separate and detect the shifted longer wavelength fluorescence light. Since the fluorescence signal is typically three to six orders of magnitude weaker than the illumination light, the challenge is to produce a high-power illumination while simultaneously and efficiently separating and detecting weak fluorescence emission. This is historically achieved by using a powerful mercury arc lamp as a light source and implementing special short-pass, bandpass, or long-pass filters and beam splitters. Modern fluorescence widefield microscopes benefit enormously from the continuous development of optics, coating, light-emitting diode (LED) and detector technologies. The availability of more than a dozen high-power LEDs provides flexible, stable and gentle fluorescence illumination. The apochromat optics and objectives correct the color shift across the entire visible light range. Advanced coating technology has pushed the filter efficiency close to 100%. State-of-the-art EMCCD and sCMOS cameras detect the faintest fluorescent signals with above 95% quantum efficiency (QE). These advances have made it possible to observe and record very challenging samples, like living cells and biomolecules in three dimensions, for a long period of time with minimum disturbance.

However, those hardware developments do not address a fundamental problem of fluorescence widefield microscopy: image degradation and optical blur caused by the light diffraction through an optical system. The ever-improved sensitivity of the hardware makes such degradation even more apparent. The model of the optical blur is based on the concept of a PSF. In a fluorescence widefield microscope, the shape of the PSF approximates an hourglass, and the size (or the level of the spread) is decided by the wavelength and numerical aperture (NA) of the objective.

The PSF serves as the basic building block of an image. Anything smaller than the PSF is not directly resolvable, regardless of magnification or pixel size. Unfortunately for fluorescence widefield microscopy, the spreading of the PSF in the axial direction is much longer than in the lateral direction. The axial extension is theoretically infinite, and it significantly limits the axial resolution. What is worse, such unwanted axial extension (or out-of-focus blur) is mixed with the in-focus signal in another layer which further reduces the SNR of the in-focus structure. Often the resulting fluorescence widefield image is associated with lower resolution, poor SNR, and reduced contrast, especially with high NA objective and thick samples. Popular optical sectioning methods such as confocal improve the resolution and contrast by physically removing such out-of-focus blurs. The hardware implementation of the laser-based point illumination and a pinhole can efficiently stop the out-of-focus blurs from reaching detection. However, this process inevitably removes a significant number of photons from the sample and reduces overall detection efficiency. Wouldn't it be better to "reuse" such out-of-focus blurs? This is what restorative widefield 3D deconvolution aims to do. Suppose we have an extraordinarily thin sample, and the optical system generates a perfect PSF, free of aberration and noise. In that case, we can mathematically reassign all the out-of-focus blurs back into the focal point with high confidence. Sadly, such a perfect imaging condition does not exist. Practically, we must deal with multiple imaging artifacts, like light scattering, spherical aberration and additional noise from the sample and camera.

The previous sections have already discussed in general how to properly acquire images for deconvolution. For fluorescence widefield microscopy, there are some additional considerations.

1) Work with thin samples only, ideally within 10 µm. Light scattering is strictly a random phenomenon. The level of scattering depends on the light wavelength (a longer wavelength has less scattering), the optical heterogeneity of the tissue and most prominently, the tissue thickness. Thick tissue significantly randomizes all signals. Without an additional mechanism to differentiate in-focus and out-of-focus signals, such as the pinhole in confocal or the grid projection in Apotome, the deconvolution photon "reassignment" is marred by error.

2) Pay special attention to image sampling and axial ranges. A fluorescence widefield image has a fixed pixel size with a given set of objectives, tube lens, camera and camera adapter. It does not have the pixel size flexibility of a confocal or a pre-calibrated configuration like in SR-SIM. The user, in many cases, is required to confirm the pixel size and the sampling manually. Most microscope software will automatically calculate and display the pixel size. Nevertheless, it is still nec-

essary to compare that with the theoretical resolution. A GFP imaging channel using a 63×/1.4 objective with a 1× tube lens, a ZEISS Axiocam 705 mono camera, and a 0.63× camera adapter all give a pixel size of 87 nm. The theoretical resolution is ~220 nm, which translates into a lateral sampling rate of 2.5× – ideal for deconvolution. The axial sampling rate can be controlled by the Z motor, and many types of imaging software would suggest an "optimal" 2× sampling. For widefield deconvolution, it is advisable to acquire axial ranges slightly above and below the physical sample thickness, about half of the axial PSF size, so that the additional out-of-focus blurs can also be utilized (see Figure 2). If a given fluorescence widefield image does not have an optimal sampling, it is recommended to use the neighbor-based algorithm like nearest-neighbor instead.

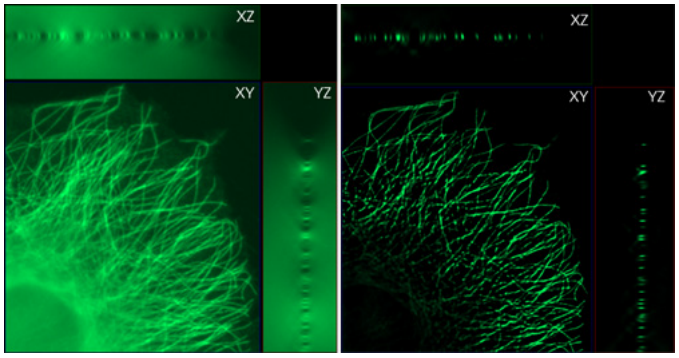

Figure 2 *Orthogonal projection of a widefield 3D dataset before and after deconvolution. The cross-section views of the raw data clearly show the presence of out-of-focus blur signals but also highlight the lack of imaging artifacts. Such a dataset is especially suitable for deconvolution. The cross-section of the deconvolved data confirms the reassignment of the out-of-focus blurs and the increased SNR.*

3) Spherical aberration can be partially corrected with a depth variance algorithm. Spherical aberration is usually caused by the wrong cover glass thickness or a refractive index mismatch between the objective immersion medium and the sample mounting medium. It leads to axial asymmetry in the shape of the PSF, and the level of the asymmetry varies at different imaging depths. During image acquisition, it is critical to match the objective immersion type with the sample mounting medium, e.g., using a water objective for live cells cultured in aqueous medium or oil objectives with fixed samples. In practice, the match is never ideal. Most commercial mounting media have a refractive index of 1.41 to 1.49, while the objective immersion oil is 1.52. Different materials also react differently to temperature variation. Some advanced objectives have a dedicated correction collar to compensate for such variation, but the procedure is usually tedious, and the correction is seldom complete. Deconvolution provides a valuable alternative to address spherical aberration for fluorescence widefield microscopy (see Figure 3). By specifying the refractive index of both immersion and embedding media, the program can simulate multiple PSFs at different imaging depths. Those multiple PSFs are then used at different depths in the raw data for deconvolution.

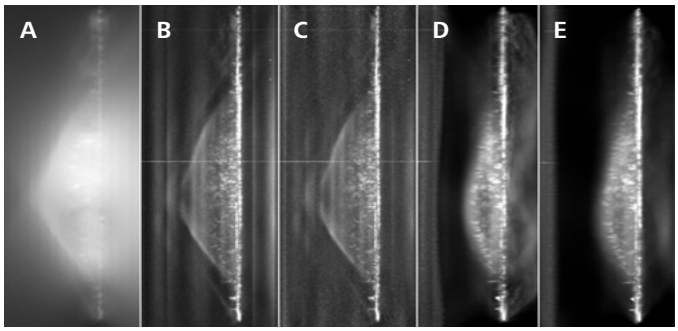

Figure 3 *Example of deconvolution improvement by additional corrections. A) a cross-section view of the raw data of a U2OS cell in PBS solution, acquired using Plan Apochromat 63×/1.4 oil immersion objective. Strong spherical aberration is present due to refractive index mismatch. B) Default constrained iterative deconvolution. C) Constrained iterative deconvolution with background correction activated. D) Constrained iterative deconvolution with background correction and aberration correction of PBS as embedding medium. E) Constrained iterative deconvolution with background correction, aberration correction, and depth variance correction with 10 PSFs. All done with ZEN Deconvolution.*

4) It is possible to perform online deconvolution. Deconvolution is computationally demanding, and the time spent on deconvolution used to be many times longer than that spent on image acquisition. Thanks to the rapid development of computer hardware, especially the GPU acceleration, the speed of deconvolution has increased dramatically. GPU-accelerated computing is the employment of a GPU to facilitate and speed the repetitive calculations of certain image processing algorithms such as deconvolution. Many commercial deconvolution software applications have implemented GPU acceleration. With a suitable NVIDIA® CUDA®-supported graphic card, ZEN Deconvolution can deliver up to 30 times faster performance than the traditional CPU-based algorithms. This speed gain makes it possible to perform online deconvolution or on-the-fly deconvolution. For example, the ZEN module Direct Processing can significantly improve usability and save time by parallelizing the image acquisition and deconvolution steps. To have the earliest possible feedback, it starts to process the smallest processable entity as soon as its acquisition has been completed. In the case of deconvolution, this is typically a Z-stack for one channel. You will be able to observe the processed result on-the-fly which is very useful for an extended time series experiment.

In summary, fluorescence widefield microscopy benefits the most from deconvolution. The hardware implementation also exploits some key advantages compared to other imaging modalities:

1. The setup is simple and can be automated efficiently for high throughput imaging.
2. The acquisition speed is fast and is only limited by the camera frame rate and sample brightness.
3. The simple beam path leads to high sensitivity.
4. It is more affordable.

With the implementation of on-the-fly deconvolution, it is well suited for imaging thin monolayer cell cultures, yeast, bacteria, thin tissues sections, C. elegans, fluorescence in situ hybridization-prepared cytogenetic sample, and many more.

Deconvolution for light sheet fluorescence microscopy

Light sheet fluorescence microscopy (LSFM) is one of the most recently introduced microscopic techniques, yet it witnessed the fastest growth in development and application in the past decade. The basic principle of LSFM is the generation of a thin sheet of light for sample illumination, with the illumination and detection decoupled at a perpendicular geometry. Contrary to the traditional epi-illumination, LSFM has an inherent optical sectioning capability. The perpendicular light sheet does not illuminate regions that are not in the focal plane, which leads to significantly less sample phototoxicity and photobleaching. LSFM, such as ZEISS Lightsheet 7, has been used widely for gentle and fast imaging of living cells, organoids, plants, and embryos over extended periods. The fast acquisition speed, large field of view, and the possibility to adapt sample holders and optics for a higher refractive index of 1.33 to 1.58 also makes LSFM the method of choice to image centimeter-sized optically cleared brains, tissues, and even entire animal models. To further improve the axial resolution, a lattice illumination pattern can be generated to replace the standard Gaussian beam, which reduces the light sheet thickness down to 550 nm. Lattice light sheet microscope, such as ZEISS Lattice Lightsheet 7, brings all the advantages of LSFM to isotropic subcellular resolution. With camera-based detection, LSFM deconvolution is similar to widefield deconvolution, but it possesses a few unique exceptions:

1. The PSF is unique. The theoretical PSF of the LSFM should be the product between both illumination and detection. If the light sheet is considerably thicker than the axial resolution of the detection objective, the overall axial resolution is dominated by the detection objective alone. This could happen by using the Gaussian beam light sheet together with high NA (>0.8) detection objectives. On the other hand, when using a Gaussian beam light sheet with low NA detection objectives or using a thin lattice light sheet, the light sheet thickness will dominate the axial resolution, and considerably influence the theoretical PSF. In both cases, the axial calibration between illumination and detection before image acquisition is critical. Even with just a few nanometers shift, the image quality can degrade dramatically. An adequately modeled PSF can partially restore such image degradation. The unique PSF can also be used to correct the lattice light sheet sidelobes. Sidelobes are common for lattice light sheet when one tries to generate the thinnest possible sheet. The presence of the sidelobes reduces imaging contrast. Deconvolution with a proper PSF model (with the sidelobes) can again be used to correct the sidelobes in the acquired data, which improves the resolution and contrast.
2. Be careful of the file size. It is well known that LSFM generates large amounts of data. A typical application could be the entire 3D volume being imaged every 5 mins for 24 hours for a zebrafish embryo, or a 10 by 10 tile imaging routine with thousands of Z-stacks for a cleared mouse brain. The file size can quickly reach a terabyte. Even with the most advanced GPU hardware, it might still take days to deconvolve one image. Practically, one might want to subset the original data to the region, time, and channel of interest before sending it for deconvolution. For opaque samples, it is also beneficial to subset limited Z ranges. For the deconvolution settings, constrained iterative would be the method of choice, but one might want to keep the iteration to a smaller number such as 10 to shorten the processing time.
3. Pay attention to LSFM-related image processing. LSFM, because of its unique beam path and sample mounting, has a few special image acquisition and processing steps, noticeably dual-side fusion, multi-view reconstruction, and lattice light sheet deskewing. The perpendicular light sheet illumination of LSFM can be introduced from either side of the sample sequentially. Such dual-side illumination gives a more homogenous result but requires an online or offline fusion of the two images. Some special dual-side fusion algorithms are nonlinear, and the results cannot be used for deconvolution. One such example is the maximum fusion, where the two images are compared pixel to pixel, and only pixels with higher intensity values are kept. Another unique LSFM image processing routine is multi-view reconstruction. Multi-view imaging is the sequential acquisition of multiple Z-stacks from different directions via sample rotation. When adequately registered and fused, multi-view imaging improves the images by combining the complementary information from each angle and achieving isotropic 3D resolution. Typically, deconvolution is only performed after the multi-view reconstruction, and the PSF model, now with a “star shape”, also needs to take into consideration the multiple PSFs at different angles. It is also possible to deconvolve each view before the registration or before the fusion, but such practices take considerably more time. The last image processing technique in the discussion, deskewing, is related to lattice light sheet only. The implementation of lattice light sheet for coverglass-based thin samples usually has a non-standard illumination angle. For example, ZEISS Lattice Lightsheet 7 illuminates the sample from 30 degrees and detects at 60 degrees. When performing a volume scan by moving the sample horizontally, the Z-stack raw data is skewed and requires an additional “deskew” transformation before visualization and analysis. The deskewing process tends to increase the file size as it fills the shifted and enlarged volume with “empty” data. For speed gain, it is necessary to execute deconvolution before the deskewing process. If one chooses to perform deskewing first, the PSF will also need

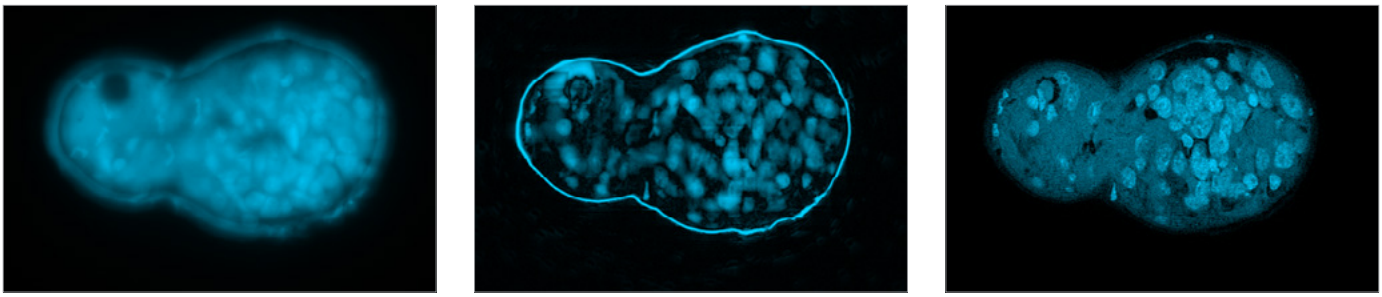

Figure 4 *Giant live fluke stained with Hoechst 33342. The homogeneous fluorescence in the inner parts of the widefield image (left) poses a serious problem for the background correction algorithms (center). Some structures remain, but generally, there are too many black spaces between the cells. This becomes visible when comparing the results to an optical section, acquired with ZEISS Apotome (right). Notably, the prominent rim around the structure, as seen in the background-corrected image in the center panel, is an artifact of interference in the widefield image, which is not seen with an optical sectioning system.*

to be internally transformed to match the geometry of the deskewed data. To simplify the workflow and avoid potentially incorrect PSFs, ZEN Lattice Lightsheet processing combines the deconvolution and deskewing steps in one operation.

Deconvolution for Apotome – reliable and easy to use

Optical sectioning allows efficient minimization of out-of-focus light to create crisp images and 3D renderings. ZEISS Apotome 3 uses a grid to generate a pattern of intensity differences. After the fluorescence of a grid position is acquired, the grid moves to the next position. If out-of-focus light is present at a certain region of the sample, the grid becomes invisible. From the individual images acquired with structured illumination, reliable optical sections can be calculated using well documented algorithms.

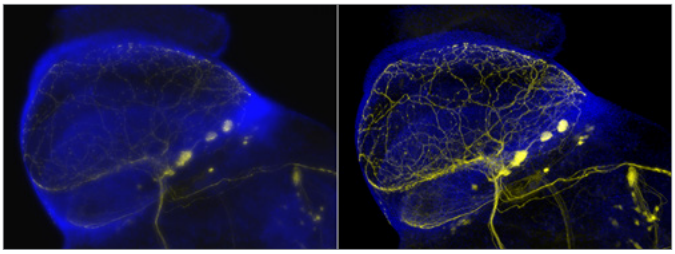

Figure 5A *Conventional fluorescence* ***Figure 5B*** *Apotome 3*

Drosophila neurons, blue: DAPI, yellow: GFP. Objective: Plan-Apochromat 20×/0.8. Courtesy of M. Koch, Molecular and Developmental Genetics, University of Leuven, Belgium

Despite hardware-based methods for creating optical sections, purely software-based solutions have emerged over the last years. As pure software solutions can use only the acquired widefield image, users must trust that these black-box solutions produce structures that are real and do not remove structures when "enhancing" the image.

Figures 4 shows a comparison of a widefield image, a background-subtracted image processed using a software algorithm and an image acquired with ZEISS Apotome. Even though the background-subtracted image shows a high contrast that is pleasing to the eye, features are missing, and structures look entirely different. Without knowing the true image, it is almost impossible to realize this. With Apotome, quantitative optical sectioning calculations can be used for a variety of samples.

Deconvolution improves the quality and resolution of images acquired with Apotome even further. Compared to deconvolution of widefield images, the patented algorithm for Apotome deconvolution uses the additional information present from the structured illumination. This allows a better reconstruction of the sample without introducing artifacts. Apotome deconvolution uses linear approaches to yield quantitative results. The signal to noise ratio is improved and a higher optical resolution can be achieved.

One of the benefits of Apotome 3 is the ease of using it. General recommendations with respect to signal to noise ratio and sampling of the specimen must be taken into account. Despite this, few additional settings need to be adjusted. The most important parameter is the number of images with the projected grid. While Apotome needs at least 3 images with the projected grid for processing of the optical section, increasing the number to 5 or 7 images can improve image quality. Further increasing the number of grid positions for an optical section does not lead to significant improvements, but it does decrease frame rate and may introduce photo bleaching.

Deconvolution with Apotome is also easy to use. By default, a theoretical PSF is automatically calculated using the information in the metadata. The strength of the deconvolution is selected automatically by the software but can be set manually, although there is the risk of introducing artifacts for settings not matching the sample and acquisition parameters. The refractive index of the sample medium and the distance to the coverslip can be set if they are known to correct for aberrations.

For calculation of the optical section, with or without deconvolution, the image can be corrected for bleaching. Local bleaching corrects the bleaching for each pixel and yields typically the best results. Alternatively, none or a global bleaching correction can be chosen. Additionally, a Fourier filter of different strength

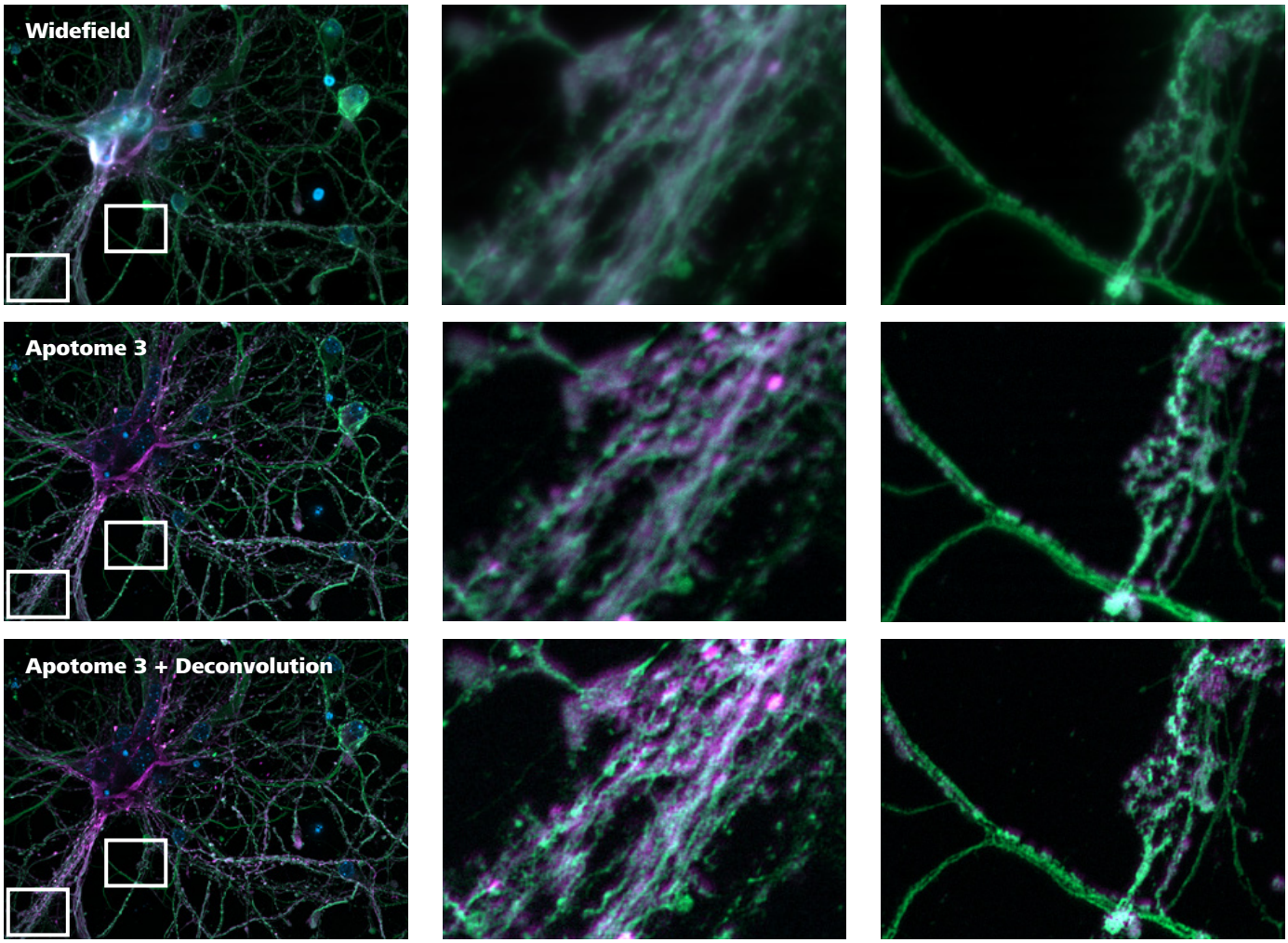

Figure 6 *Cortical neurons stained for DNA, microtubules and microtubule-associated proteins. Courtesy of L. Behrendt, Leibniz-Institute on Aging – Fritz-Lipmann-Institut e.V. (FLI), Germany.*

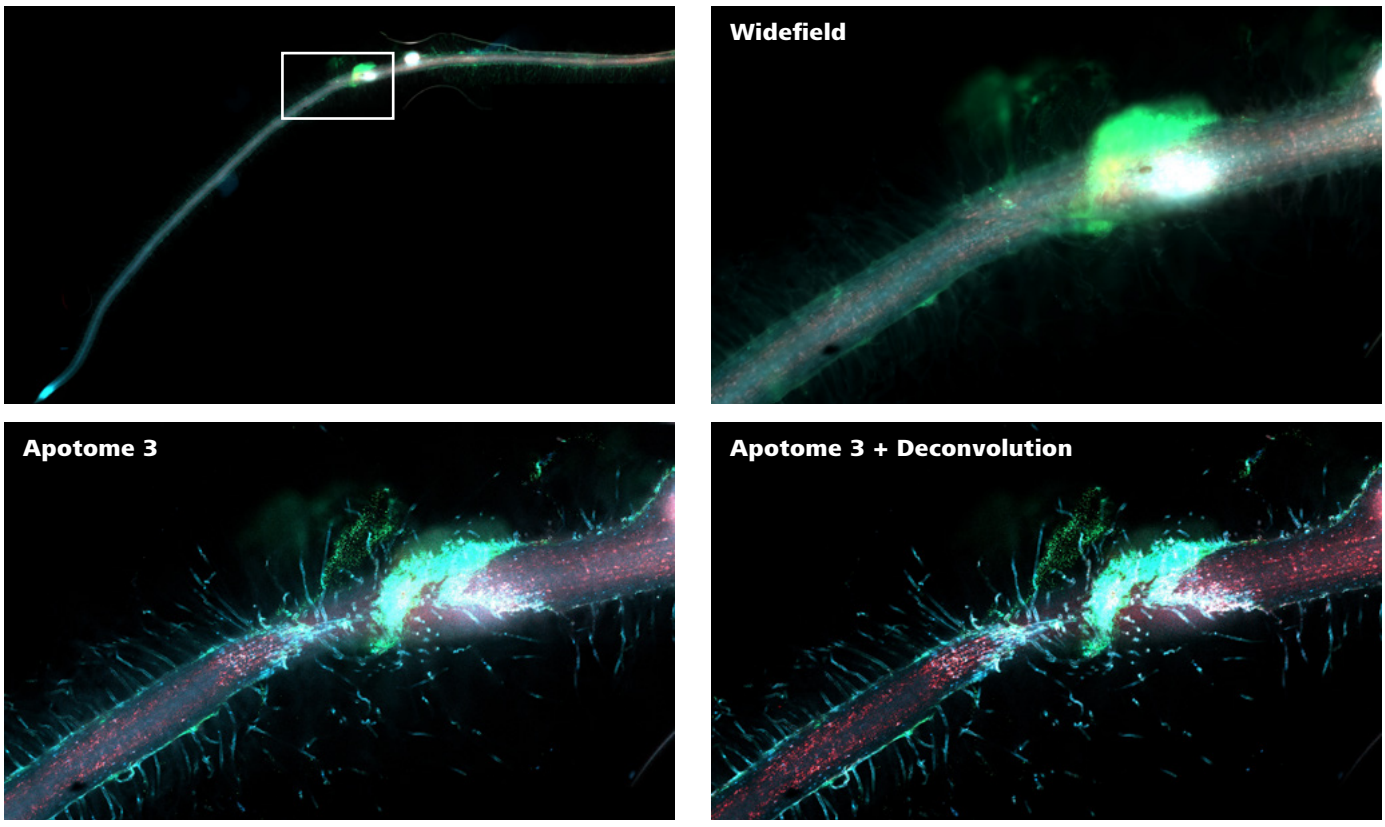

Figure 7 *Autofluorescence of a Lotus Japonicus root infected with symbiotic bacteria stained with mcherry. Courtesy of F. A. Ditengou, University of Freiburg, Germany.*

can be used if remaining stripes happen to be present in the image. Bleaching and Fourier filter correction also can be combined if necessary.

When using Apotome deconvolution in the processing function of ZEN, additional processing options are available, but typically they are not required. These corrections are not Apotome-specific and can be applied to other deconvolution methods, too.

To remove offsets, the background subtraction option can be used to subtract the intensity of a smoothed average. If light sources having a non-constant light output were used for image acquisition, flicker correction can be implemented. State of the art LED light sources typically do not suffer from flickering and their usage improves the data quality during acquisition. The pixel correction function replaces the bad pixels that cameras can have by considering the mean value of the neighboring pixels. State-of-the art CMOS cameras like ZEISS Axiocam designed for scientific applications and typically have only a few if any, bad pixels. The fluorescence decay correction compensates for bleaching during a Z-stack. If bleaching is present and not corrected, it significantly alters deconvolution results. This option uses the average intensity of the individual slices of the Z-stack to correct for bleaching and improves the deconvolution results for Z-stacks with noticeable bleaching, thereby improving the deconvolution result for this type of data.

Even though a 2D deconvolution can be applied to Apotome images, 3D deconvolution improves the results because more information is available. Figure 6 and 7 show examples of wide-field, Apotome and Apotome + deconvolution images showing the increase in image quality and resolution.

Confocal Deconvolution – LSM Plus

The history of deconvolution for confocal data is rather long, but the history of truly embedded and tailored deconvolution in confocal systems is rather short. The advances in development have taken place only in the last few years. At ZEISS, these advances have produced the new LSM Plus configurations of the LSM 900 and LSM 980.

In the last 10 years, ZEISS has developed two major improvements to their confocal instruments: parallel spectral detection, represented by the Quasar (Quiet Spectral Array) detector design, and resolution and speed detection, represented by Airyscan. For both, ZEISS implemented parallelization in acquisition as a tool to boost SNR and minimize sample stress. This fulfills a dream voiced by many users to combine these detection methods in confocal instruments. This also was one of the catalysts for the LSM 9 series, introduced in 2019, which provides the first implementation of these developments.

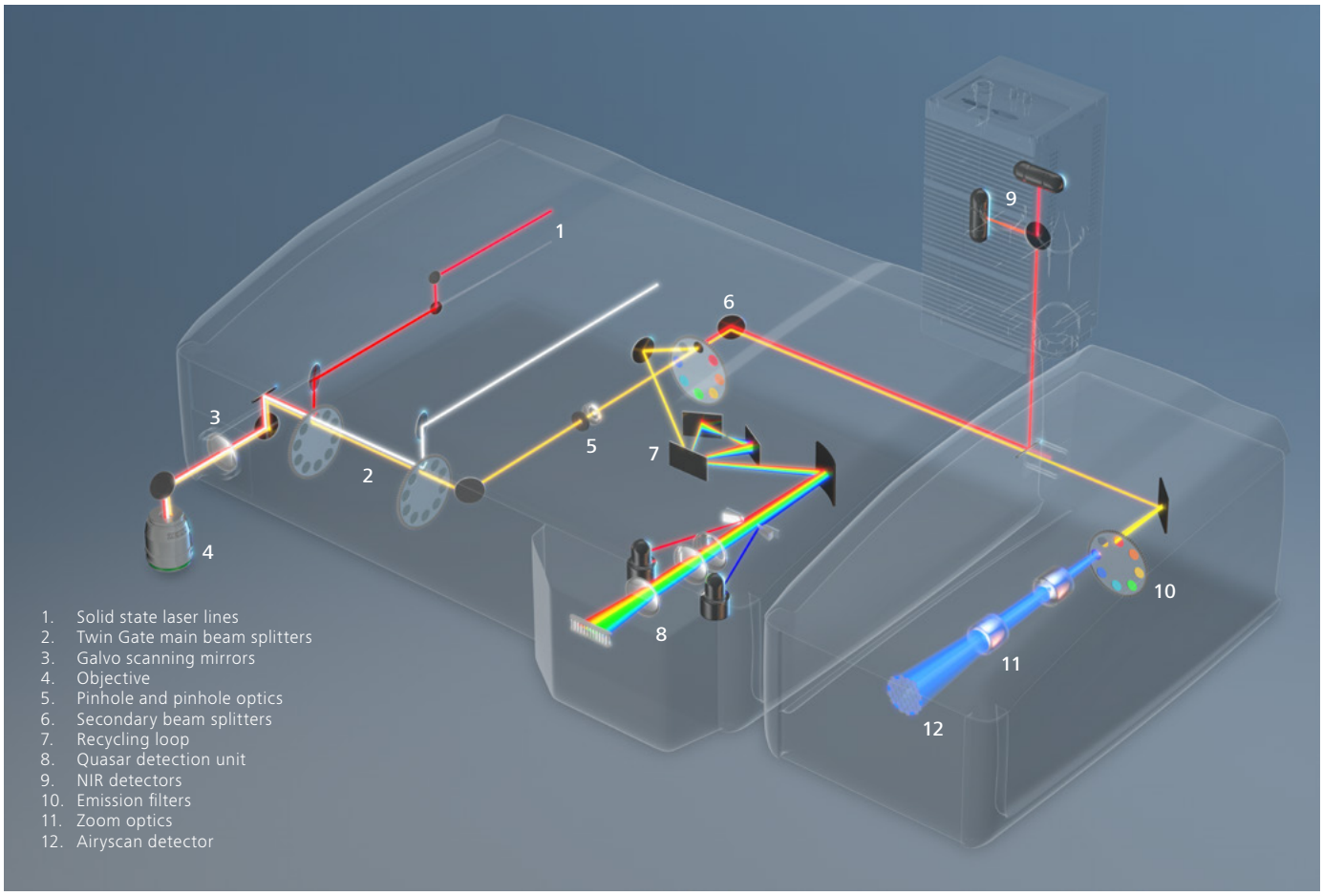

Figure 8 *Beam path of LSM 980 with Airyscan 2 and NIR detection*

In 2021, ZEISS has made a big step in the direction of embedded and tailored deconvolution as an important technology with the release of the new LSM Plus. So, what was done here exactly? Spectral detection advanced from 32 channels (8 with 4 read-outs) to 36 channels. Wider data bandwidth including Online Fingerprinting, and GaAsP cathode technology also contributed to increased versatility in the few last years. This meant a more cost effective 6-channel solution in 2018/19, and a more powerful 36 channel solution, including special NIR detector channels, in early 2021, all integrated in the same proven lambda stack and spectral unmixing workflow.

Figure 9 *Spectral detection GUI, integrating several detector types which can be used with LSM Plus.*

The Airyscan detection developed from SIM-like super-resolution with improved SNR, to parallelized fast super-resolution, and advanced to instant 2D enhanced processing (2D SR mode for single plane acquisition), faster processing for big data (4-ring format) and even faster sensitive acquisition (8× parallelization MPLX mode). All these methods are based on an embedded tailored deconvolution on the processing side, which includes the mathematical steps of a weighted Sheppard Sum generation (Sheppard 1988), exact PSF modelling for the ZEISS LSM and a linear quantitative Wiener deconvolution. All this can run in real-time with a preview and has just one strength control parameter which even can be automated.

Bringing both technologies together was a challenge for ZEISS, since both features produce large amounts of data per acquired pixel. Consider spectral detection with up to 36 channels, and Airyscan with 32 elements. This would have resulted in 36×32, totaling 1152 channel elements for each pixel, a data load that exceeds any readout electronics on the market now and in foreseeable future. So, if spectral Quasar detection cannot fully come to Airyscan, can some Airyscan maybe come to Quasar? That indeed was the breakthrough that ZEISS started to develop two years ago, and which became a product in 2021, as the LSM Plus function for all ZEISS LSM 900 and 980.

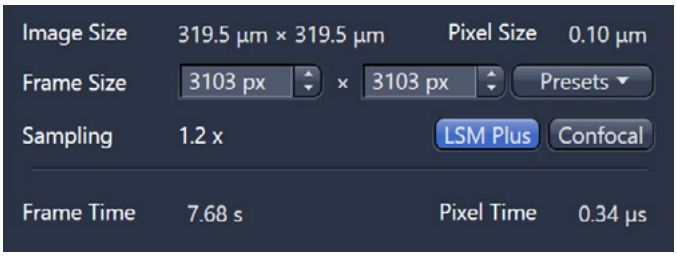

Figure 10 *LSM Plus function with optimized acquisition settings. Sampling is set automatically and interlinked with the pinhole setting.*

LSM Plus utilizes processing components from Airyscan, in the form of the exact PSF modelling for the ZEISS LSM and the linear quantitative Wiener deconvolution, applied to the current 36-channel, NIR capable Quasar detection. LSM Plus can again run in real-time with a processing preview, and has just one control parameter, which again can be automated. Instant Online Fingerprinting function was also improved by adding the side PMTs of the Quasar and the NIR detectors, the optimized workflow, and the capability of LSM Plus processing, even in its most automated way – with Direct Processing using Auto processing strength. Though LSM Plus works with all detectors, including non-descanned detectors (NDD) for multiphoton imaging, it is not limited to use on very expensive systems. It also benefits a 2-channel ZEISS LSM 900.

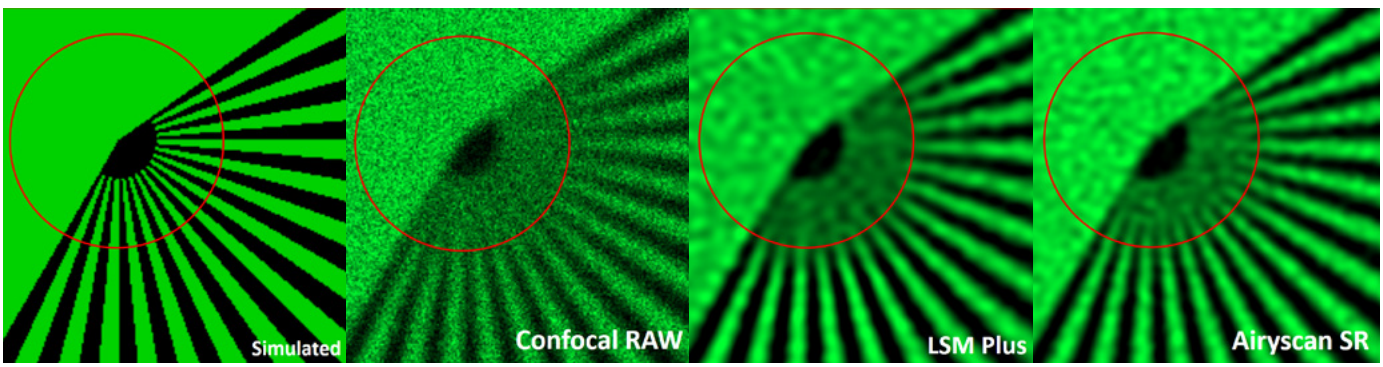

Figure 11 *Resolution limits of Confocal, LSM Plus (Confocal Wiener DCV), and Airyscan SR detection. In addition to the resolution gain, both Airyscan and LSM Plus reduce noise and improve visibility.*

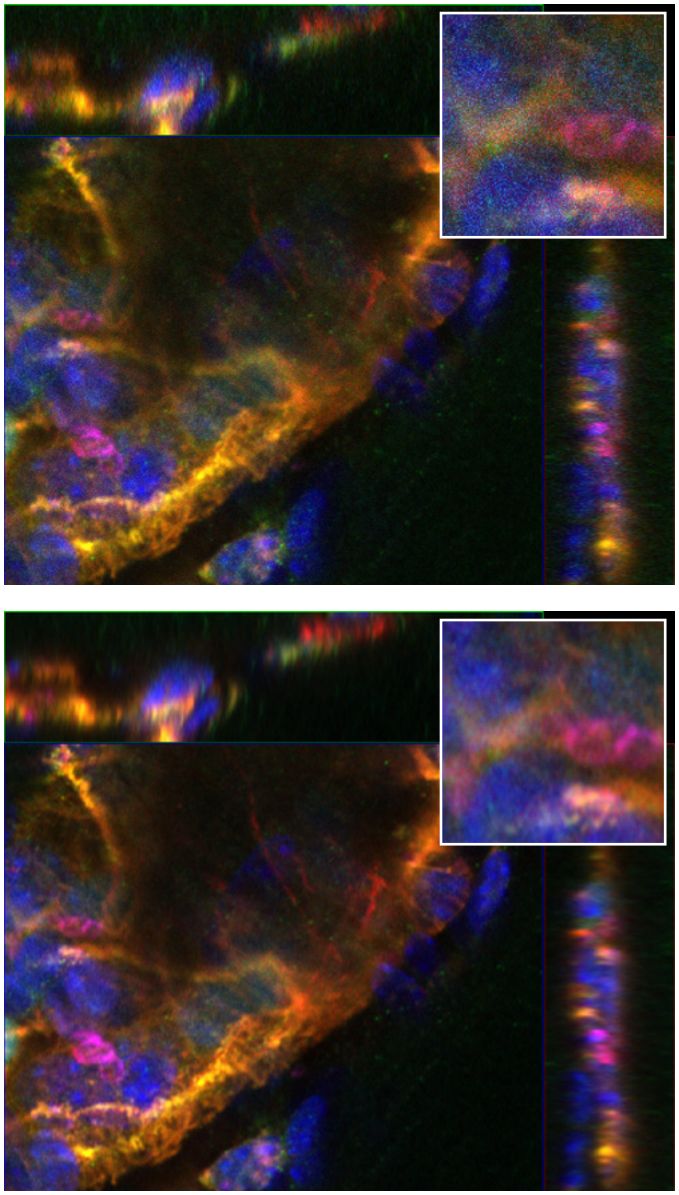

Figure 12 *Murine cremaster muscle, multi-color label with Hoechst (blue), Prox-1 Alexa488 (green), neutrophil cells Ly-GFP, PECAM1 Dylight549 (yellow), SMA Alexa568 (orange), VEGEF-R3 Alexa594 (red), platelets Dylight649 (magenta). Acquired with 32-channel GaAsP detector using Online Fingerprinting on ZEISS LSM 980, without (top) and with LSM Plus (bottom).*

Sample courtesy of Dr. Stefan Volkery, MPI for Molecular Biomedicine, Münster, Germany

Additionally, there is a true collaboration between Quasar and Airyscan when using the multitracking mode. Here, Airyscan becomes an additional channel in the spectral acquisition setup, providing extra high resolution in addition to the LSM Plus processed channels. More than 40 data channels are processed in this mode, and after the deconvolution steps of Airyscan and LSM Plus, the resulting channels can undergo a spectral unmixing for perfect dye separation. By closing the pinhole in the LSM Plus channels, the resolution can be pushed further to get an optimal match to the Airyscan channel.

What are the technical capacities of LSM Plus, and what is the deconvolution behind it?

Resolution	Confocal	LSM Plus e.g. 0.8 AU	LSM Plus e.g. 0.3 AU (closed PH)	Airyscan SR* (1.25 AU)
X/Y	250 nm	160 nm**	120 nm**	120 nm**
Z	700 nm	500 nm	500 nm	350 nm
Spectral range	380–900nm	380–900 nm	380–900 nm	400–750 nm

*without Airyscan jDCV;
**measured with Nanoruler DNA Origami samples 160 nm/120 nm spacing

What's behind the LSM Plus processing?

The calculation used for LSM Plus is based on the Airyscan Wiener Filtering, but with the use of just one channel and the PSF for the confocal image. This yields all the advantages of this calculation like fast linear processing and online preview. The processing is quantitative and uses just one strength parameter, which is set automatically to a suggested best fitting value.

The size of the pinhole is an additional parameter which influences the representation of frequencies and the maximum possible resolution. A smaller pinhole results in higher spatial frequencies and therefore higher usable sampling rates which positively contribute to the achievable resolution. Closing the pinhole of course requires enough signal from the sample.

The resolution gain of LSM Plus can be higher than the usual DCV factor of 1.4. The reason for this is the quality of the optimized PSF models, which can adjust to the instrument properties in the same way as with Airyscan. Another advantage is the robustness of the Wiener filtering used here, which is applied in the event of image noise or aberrations. Such a mismatch does not create annoying artifacts, but it does reduce the maximum resolution which can be achieved. The perceived SNR is always better with LSM Plus, even with non-optimal samples.

LSM plus offers an embedded and optimally tailored deconvolution which improves the spectral detection properties of ZEISS LSM 980 and ZEISS LSM 900 and complements other features of the LSM, like NIR detection, Online Fingerprinting, multiphoton imaging or Airyscan.

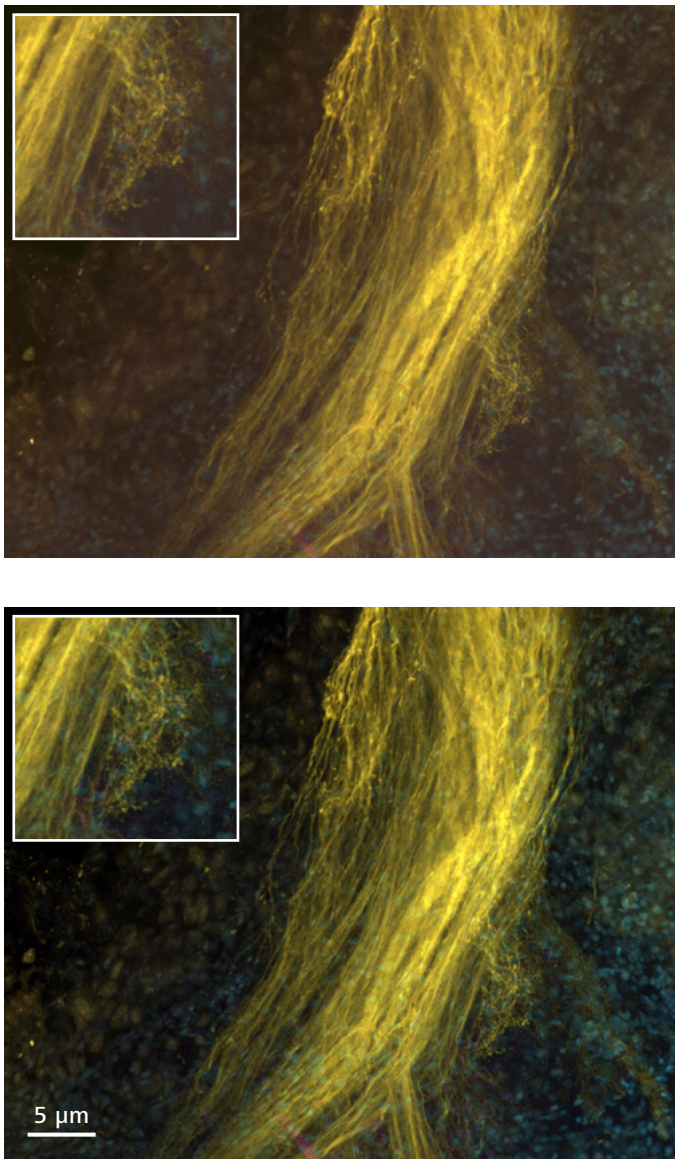

Figure 13 *Cockroach brain neurons (Alexa 488: yellow, Alexa 647: magenta) and DNA (Hoechst: cyan), without (top) and with LSM Plus (bottom). Sample courtesy of M. Paoli, Galizia Lab, University of Konstanz, Germany*

Step by step to 90 nm – Airyscan Joint Deconvolution (jDCV)

ZEISS Airyscan features a 32-channel gallium arsenide phosphide photomultiplier tube (GaAsP-PMT) area detector that collects a pinhole-plane image at every scan position. Each detector element functions as a single, 0.2 AU pinhole where the data from each element carries not only intensity information but light distribution and location information. In total, 1.25 AU is collected by the whole detector. The 0.2 AU of each element determines the sectioning and resolution in XY and Z, whereas the 1.25 AU determines the sensitivity. By shifting all the images back to the center position, which can be done easily since the amounts of their displacements are known, an image called the "Sheppard sum" is generated. This image has a 1.4× higher resolution compared to that of a classical confocal image.

The classic Airyscan Processing, which includes the linear Wiener filtering, leads to a simultaneous increase of 4–8× in signal-to-noise as well as a two-fold spatial resolution improvement over classical confocal. Thereby, the choice of the Wiener noise filter will balance between higher resolution and better SNR in the image. Changing the Wiener filter parameter results in the selection of different frequency bands and their individual amplification. The signal of each detector element is deconvolved separately and the contribution of each detector element is weighted. This allows a robust DCV with the positional information of the detector elements also considered, leading to a resolution of 120 nm laterally and 350 nm axially for 488 nm excitation.

Since its introduction back in 2014, Airyscan has continuously improved over time, enabling for example 120 nm lateral resolution without acquiring a Z-stack with the 2D SR super-resolution mode. This mode takes advantage of the fact that the confocal point spread function entangles information from X, Y and Z planes in the pinhole plane. Airyscan can measure the emission fluorescence distribution in a single image acquisition, thereby yielding information about how the signal is entangled. The algorithm of the 2D SR super-resolution mode makes it possible to distinguish and separate the light originating in the focal plane from light originating outside of the focal plane. The evolution of Airyscan has continued and in 2019, ZEISS introduced Airyscan 2 and the Multiplex mode. Multiplex mode handles image data in a way that reduces data size and improves reconstruction times, addressing the need to capture structural dynamics, cellular signaling, molecular trafficking and diffusion events with real-time super-resolution and superior SNR. Instead of carrying 32 elements of information per pixel, improved data handling schemes allowed a new preprocessing step where the information from the 32 elements is transformed into 4 "rings" of information per pixel. The change in data structure leads to a 6.6× decrease in raw data size and improves processing time by a factor of 5×.

The new Airyscan jDCV Processing, in contrast to the classic Airyscan Processing, features an accelerated joint Richardson–Lucy algorithm, supporting Airyscan raw data images as well as ring-preprocessed images. Taking advantage of the unique Airyscan concept including light distribution and location information from the pinhole plane of each detector element, this "multiview-information" is used to achieve a better reconstruction result, especially for noisy and low SNR images, in comparison to the Wiener filter implementation in the classic Airyscan processing. A better statistical interpretation and additional a-priori information (noise distribution and non-negativity) are leading to a sample-dependent resolution improvement down to 90 nm. This makes information available which has not been accessible previously, for example spine-distribution and morphology for quantifications (Figure 14). These benefits can be extended to multiphoton excitation to gain significant improvements in resolution and SNR.

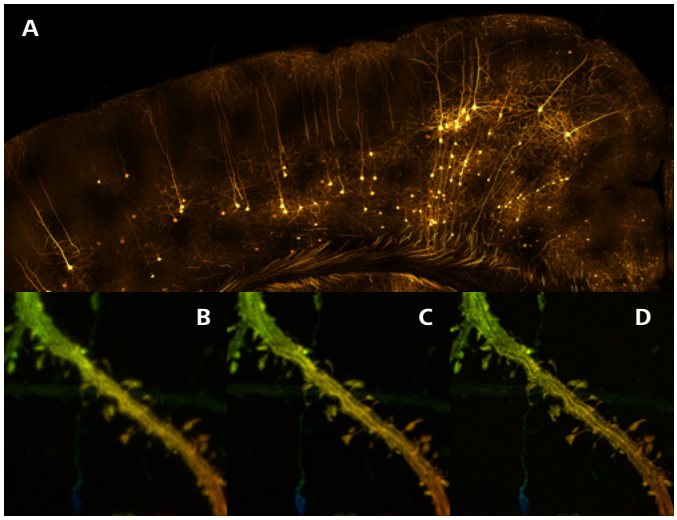

Figure 14 *Murine brain expressing the neuronal marker Thy1-eGFP, imaged on an LSM900 with the Airyscan 2. A: Multiplex mode SR-4Y, Plan-Apochromat 20×/0,8 NA over a Z stack range of 14 µm brain cortex and displayed as a maximum intensity projection. Comparison; B: Confocal, 1 AU, Sampling 1.0×, Z stack range of 11 µm; C: Airyscan SR, Sampling 2.0×, Z stack range of 11 µm, classic Airyscan 3D Processing, Strength 5.0; D: Airyscan SR, Sampling 2.0×, Z stack range of 11 µm, Airyscan Joint Deconvolution, Maximum Iterations 20) of the highlighted FOV and displayed as a color-coded maximum intensity projection.*

Only two parameters need to be considered in the new Airyscan jDCV processing:

1. Maximum Iterations, which can be either selected by available presets in a dropdown list (Dense, Standard and Sparse) or freely selected with a slider. In cases of more than one fluorophore, the checkbox "Adjust per channel" is available and the iterations can be selected individually for each fluorophore. "Start with Last Result", which is available after the initial first processing, saves intermediate processing results and allows initiation of the processing based on the last calculated iteration.
2. Quality Threshold represents an alternative "stop criterion". Iterative DCV processing stops when the difference in fit quality between most two recent iterations is smaller than the quality threshold value.

The constant development effort is pushing the boundaries of Airyscan once more, starting with 140 nm lateral resolution back in 2014, 120 nm lateral resolution without acquiring a Z-stack in 2018, and now achieving resolution improvements down to 90 nm for 488 nm excitation. At the same time, signal-to-noise has increased 4–8× and it is now possible to achieve rapid volumetric imaging in the Multiplex mode for Airyscan 2. More importantly, this technology is easy to use and available for everybody with a couple of clicks in a simple processing GUI.

SR-SIM with iterative DCV: imaging at 60 nm resolution

Super-resolution structured illumination microscopy (SR-SIM) is a well-established tool for fast and flexible multi-color imaging beyond the diffraction limit. Typically, SR-SIM systems are wide-field camera-based microscopes and they double the resolution of conventional imaging systems. But using iterative deconvolution methods can further increase the resolution down to 60 nm [SIM_01]. In SR-SIM systems, the structured illumination interferes with the sample resulting in so-called Moiré fringes. Moiré fringes encode the super-resolution information of the sample but are rather large-scale structures. Thus, the high-frequency information of the sample is shifted to the frequencies detectable for the used objective. To achieve super-resolution, the sample is imaged at different positions (phases) of the illumination pattern. These phase images are then deconvolved into the resulting SR image [SIM_02]. Thus, deconvolution is inseparably linked to SR-SIM.

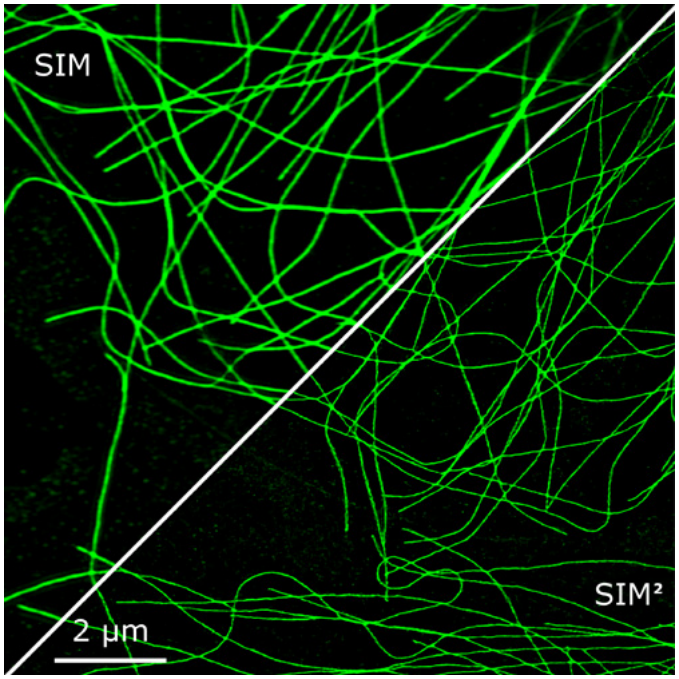

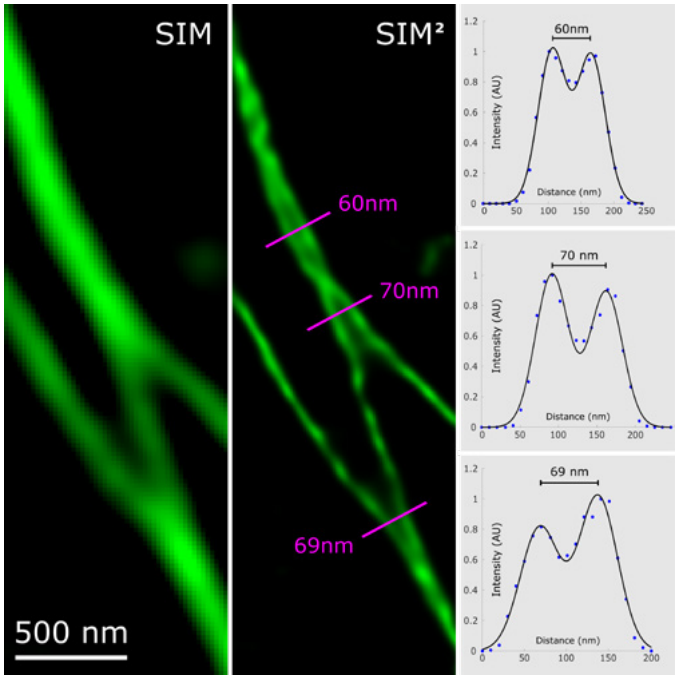

Figure 15 *Images of Cos-7 cell stained with anti-alpha-Tubulin Alexa fluor 488 were processed with the conventional SIM algorithms based on generalized Wiener filter and with the SIM² reconstruction. The images show an improvement of resolution for SIM² compared to SIM. The superior sectioning capability of SIM² is shown in the movie. Objective: Plan-Apochromat 63× / 1.4 Oil*

Optimizing SR-SIM systems mainly means increasing the quality of the image reconstruction. This can be achieved by improvement of the encoding of the high-resolution information during image acquisition and of the decoding during deconvolution. On the encoding side, using the 2D lattice illumination, as implemented in ZEISS Elyra 7, leads to higher modulation contrast and improved image quality compared to conventional 1D stripe pattern SIM systems [SIM_03]. Moreover, in contrast to the stripe illumination, lattice illumination does not require rotational movement and, thus, enables fast image acquisition. The increased efficiency of the lattice illumination is also very gentle in terms of phototoxicity, making Elyra 7 Lattice SIM a live-cell imaging system. The user of the Elyra 7 has the flexibility to choose between 13 or 9 phase image acquisition.

For achieving the highest resolutions, 13 phase images are recommended. When live samples of high dynamics are investigated, 9 phase images might be advantageous due to the increased frame rates. It is important to mention that both modes perform 3D super-resolution microscopy, even when images are acquired only in 2D. In general, it is fully sufficient to acquire images only within the sample. The user can easily identify the sample area by visibility of the illumination pattern. For optimal performance of the Elyra 7, it is recommended to use only 10 – 15% of the full grey value range, i.e., intensities of up to 6000 – 8000. For dimmer samples, it is advantageous to reach at least 100 – 200 grey values above the background noise.

On the decoding side, image reconstruction consists of multiple steps: order separation, parameter estimation, Fourier filtering, order shifting (and weighting), order combination and deconvolution. Commonly, SIM reconstruction algorithms are based on generalized Wiener filtering and the order combination and deconvolution are performed in a single step.

Generalized Wiener filtering is a linear process leading to fully quantitative results and can be carried out at high speeds. In Elyra 7, Wiener filtering is referred as SIM processing. The user can easily reconstruct the images by choosing between different strengths (weak, standard, strong) of deconvolution according to the signal-to-background levels of the acquired raw data or manually define the strength value. Nevertheless, generalized Wiener filter has certain limitations: a) The achievable lateral and axial resolutions are limited to two-fold improvement, b) Over-processing artifacts occur in low signal-to-background data and c) No iterative deconvolution can be used [SIM_01]. The first two limitations result from the non-optimal PSF used during the image reconstruction. Briefly, the microscope PSF used for Wiener filtering does not reflect the changes applied during the first steps of the processing. Thus, it is beneficial to decouple the SIM processing and deconvolution steps and adjust the PSF. Insufficiency of improving only the DCV by implementation of iterative approaches has been demonstrated in multiple cases [SIM_04, SIM_05]. Thus, ZEISS Elyra 7 contains a two-step SIM² image processing, where, in a first step, SIM processing is performed not only on the raw images but also on the microscope PSF. The resulting SIM-PSF is then used for the subsequent iterative DCV. This way, SIM² can double the conventional SR-SIM resolution in XY and improve the sectioning quality (Figure 15). Furthermore, SIM² is much more robust against overprocessing artifacts. The implementation of the SIM² algorithms in ZEN software is as easy as performing conventional SIM processing. Based on the signal-to-background quality of the raw data, the user can choose one of the default parameters, Weak, Standard or Strong, for fixed and live samples. An extra mode exists for reconstruction of large homogenous structures such as nuclei, cells expressing free fluorophores, etc. For interested users, manual adjustment of the deconvolution parameters such as Number of iterations, Regularization weight, Input SNR and Sampling is also accessible to maximize the SIM² performance. But we strongly recommend performing the default processing first.

In summary, SR-SIM is a fast, live-cell compatible imaging technique able to double or quadruple the resolution depending on the deconvolution method used.

FAQ: Deconvolution

Is deconvolution quantitative?

A quantitative method is defined here as: in the pre- and post-deconvolved image the sum of all intensities (excluding intensities that are not collected) is preserved. In a nutshell, some deconvolution algorithms are quantitative. Deconvolution algorithms generally can be categorized into three groups: neighbor-based, inverse-based, and iterative-based. Neighbor-based algorithms, also known as deblurring methods, are fundamentally subtractive in nature. They seek to estimate the contribution of out-of-focus signals in each frame and remove it.

Neighbor-based algorithms are qualitative only. Inverse-based algorithms, including the famous Wiener Filter, are linear restoration methods that are applied in a single operation. Inverse-based algorithms usually involve specific “regularization” to deal with noise, but the overall process is strictly linear and quantitative.

Iterative-based algorithms, in an over-simplified view, are a repetitive comparison operation between a current forward model result and the measured data. Each repetition’s result is applied with meaningful “constraints” and the previous output is used as the next estimate until a suitable result is achieved. For raw data with decent signal to noise ratio (SNR), iterative-based algorithms, are designed to be quantitative, no matter if they contain linear or non-linear computational components.

How does DCV exceed optical resolution?

In principle, deconvolution (DCV) is an image processing technique that seeks to reassign out of focus or blurred light to its proper in-focus location or to remove it entirely. Using this procedure, the signal-to-noise ratio (SNR) as well as the signal-to-background ratio (SBR) or even the contrast of the image will be improved. But how can resolution be improved even beyond the attainable optical resolution of the microscopic technique used for image recording?

If the image is modelled as a convolution of the object with the point-spread-function (PSF) then theoretically, the DCV of the raw image should restore the object. However, given the fundamental limitations of any imaging system and image-formation models, the best one can get is an estimate of the object. Convolution operations are best computed by the mathematical technique of Fourier Transformation, since in Fourier or frequency space convolution is just the product of the Fourier transform of the PSF, the so-called optical transfer function (OTF), with the Fourier transform of the image. The resulting Fourier image can then simply be back transformed into real space. And this brings us back to the resolution question.

The higher the frequencies are that are supported by the OTF, the higher will be the resolution in terms of distances in the restored image. Noise, however, contains the highest frequencies, so many algorithms use an approach termed regularization to avoid or reduce noise amplification. If it is possible to make assumptions about the structures of the object that gave rise to the image, it can be possible to set certain constraints for obtaining the most likely estimate. For example, knowing that a structure is smooth results in discarding an image with rough edges. A regularized inverse filter, like Wiener filter, uses exactly that approach. By this method, high frequencies arising from structures that would otherwise be obscured by high noise frequencies become available and the resolution will be improved. However, such a linear approach only would be able to achieve the theoretically possible resolution of the optical system. Or in other words, resolution is restricted to the support of the OTF. So, what about then surpassing the optical possible resolution?

This can be achieved by constrained iterative algorithms that improve the performance of inverse filters. As their name implies, they operate in successive cycles. Usually, constraints on possible solutions are applied that not only help to minimize noise but also increase the power to restore the blurred signal. Such constraints include regularization, but also other constraints like nonnegativity. Nonnegativity is a reasonable assumption as an object cannot have negative fluorescence. Such algorithms not only raise the high frequencies of the OTF support, but in addition they are able to extend the OTF support. And that in turn means higher frequencies than those transported through the optical system and therefore, higher-than-optical achievable resolution.

How much can I improve resolution with deconvolution?

It is difficult to put a number on it. Nevertheless, it is sometimes claimed that up to 2 times better resolution can be achieved with deconvolution. Contrary to popular belief, microscopy resolution cannot be straightforwardly measured. The most accepted standard to measure resolution is based on a so-called Rayleigh Criterion. Here, the smallest resolvable detail is defined when two point-objects are so close together that the center maximum of one point's Airy Disk falls on the first minimum of the others. Practically, a particular sample of either two point-objects (such as Gattaquant Nanoruler) or two line-objects (such as Argolight calibration slide) with specified distances is measured to confirm the resolution.

Another simplified and commonly used method is to measure the full width at half maximum (FWHM) of a sub-resolution object. A profile measurement across the center of an Airy Disk approximates a Gaussian curve (a Bessel function to be precise), and the resolution is defined as the length of the FWHM of the Gaussian curve.

Iterative-based deconvolution seems to enjoy some advantage of resolution improvement, especially for samples with small and clearly defined structures, and the resolution is measured with the FWHM method. Suppose you have a bright and low-density 100-nm fluorescent beads sample and use iterative-based deconvolution with strong strength and more iterations.

In that case, you can quickly obtain an alleged FWHM resolution of less than 100 nm. Determination of resolution improvement in real biological samples with complicated structures is even more challenging. Deconvolution over-processing is strongly associated with artifacts and should always be avoided for biological sample data.

Lastly, the potential resolution improvement is only achievable when the raw data is properly, or to some extent overly, Nyquist sampled. In summary, deconvolution does improve resolution, but we shouldn't blindly put a number on it and expect the same outcome every single time.

Can I do deconvolution on 2D images?

Yes. While Deconvolution yields the best result for optimally sampled 3D stacks, you can perform deconvolution on a single 2D image. However, you cannot use the nearest-neighbor algorithm, which requires neighboring frames above and below. If you use ZEN, it is recommended to use the "Deblurring" method for 2D images.

Should I use theoretical PSF or measured PSF?

It depends. There are pros and cons to both methods. Theoretical PSF can be generated automatically by the files' metadata and can easily accommodate various image inputs, e.g., data acquired with different objectives or wavelengths. Theoretical PSF is inherently noise-free and can adapt spherical aberration by using different PSFs at different imaging depths (depth variance implementation in ZEN). However, theoretical PSF assumes perfect hardware and experiment conditions that are seldomly realistic. Those non-optimal imaging conditions lead to deconvolution artifacts. Measured PSF, on the other hand, should represent the "real" PSF and include all possible aberrations (except for some SR techniques). But in practice, measured PSF (obtained by imaging and averaging sub-resolution fluorescent beads; please refer to "How is a measured PSF generated?") requires a considerable amount of effort, and the result is usually very noisy. Measured PSF is also less tolerant to spherical aberration, typical for thick samples or samples not directly attached to the cover glass. Lastly, measured PSF represents only the current microscope conditions when the beads image is acquired. These conditions, like optical alignments, lamp flickers, detector noises, and room temperature, can easily change over time. Such changes unavoidably influence the PSF and make the measured PSF not so "real" anymore. In practice, it is best to start with theoretical PSF. If the result is not satisfactory and resources are available, then you can proceed with the measured PSF.

How is a measured PSF generated?

Using a measured PSF potentially can improve the deconvolution result, especially with data acquired using high NA objectives (NA>1.2). PSF measurement is also an excellent approach to evaluate the current optical condition of your microscopes and should be carried out regularly. However, the procedure is daunting to most first-time users, and it requires proper preparation and practice. This section provides a brief guide on how to generate a measured PSF.

1. It all starts with good sample preparation. We typically use well-separated and sub-resolution fluorescent beads, prepared at the same imaging condition as used in the raw data. Bead size must be considered first. Ideally, the diameter should be slightly smaller than the physical resolution of your microscope, e.g., for a 1.4 NA objective and GFP channel, a bead with 150 nm diameter is recommended. Keep in mind that smaller beads are more challenging to locate, have weaker signals, and can be more easily photobleached. Different sized and multicolored fluorescent beads can be commercially purchased for example from Polysciences or Invitrogen. Second, the density of the beads needs to be controlled properly. Ideally, it should be a single layer of beads with minimum overlap when the beads are defocused (see Figure 16). Practically speaking, you can sonicate and dilute the beads' stock solution to multiple concentrations in ethanol and drop 3–5 of them onto the same cover glass, then let them air dry. Lastly, the beads should be prepared with the same imaging conditions of your raw data. This includes using cover glass and identical mounting medium, sample depth, and temperature. Note that it is beneficial to have an antifade agent in the mounting medium.

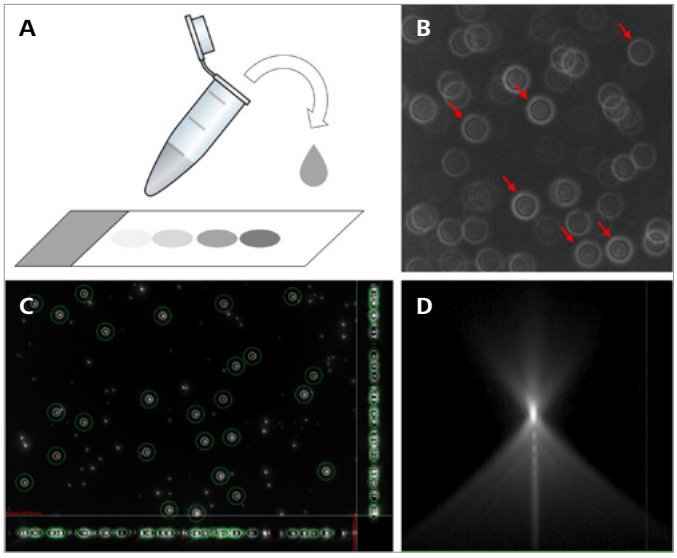

Figure 16 *An illustration to generate a measured PSF. A) drop different concentrations of sub-resolution beads solution onto a high quality 170 µm cover glass (#1.5) and air dry. B) properly adjust sample tilting, find an area where you can clearly identify well separated beads when defocused, set camera exposure to fill >50% dynamic range, define lateral and axial sampling rate ideally beyond Nyquist, acquire a z-tack until the disappearance of the out-of-focus signals. C) use a software tool to perform beads selection and average. D) save your measured PSF with a proper name.*

2. Acquire the image at the exact hardware settings. After leveling the beads sample onto the microscope stage, it is critical to use the same hardware settings as in the raw data: objectives, correction collar settings, immersion medium, light source, filters, and other unique settings such as confocal pinhole size. You can use the same lateral and axial samplings as in the raw data (Nyquist sampling or better is required), but sometimes it is advisable to set the sampling rate slightly over the Nyquist requirement. Dynamic range is important here since you need to record both bright in-focus and dim out-of-focus signals. It is recommended to use 12 bit or higher detector settings and fill at least 50% of the histogram. Lastly, when defining the Z-stacks, make sure to capture enough spaces above and below the beads until the ring signal disappears.

3. Evaluate, process, and save your measured PSF. Once the PSF measurement is done, you should first examine and assess the PSF quality using the orthogonal viewing tools. The PSF should be clear, straight, and symmetrical. If the PSF shows significant artifacts, such as tilting or uneven diffraction ring patterns, it is sensible to inspect the optical components of the microscope and redo the beads imaging. Spherical aberration cannot be fully corrected, so slight axial asymmetry is acceptable. PSF from a single bead usually has a high level of noise. It is necessary to average multiple beads to improve SNR. The ZEN Deconvolution software package has dedicated beads averaging tools. Follow the software wizard, choosing single and well-separated beads to form the final measured PSF. Lastly, save the measured PSF with a detailed description of the date, objectives and wavelength. The metadata should contain all necessary parameters, but you don't want to assign the wrong PSF to your raw data. Since the optical alignment and hardware conditions vary over time, it might be a good practice to update the measured PSF regularly.

Should I deconvolve all my microscopy images?

If you have the resource and the technical know-how, you probably should. Deconvolution is proven to improve image quality. You can expect better contrast for 2D images or for 3D images with non-optimal sampling using neighbor-based methods. For optimally sampled 3D images, using inverse-based or iterative-based methods can increase resolution and SNR. If you carefully control the parameters, deconvoluted images remain quantitative. The only drawbacks are the long processing time, possible deconvolution artifacts, and duplication of data. Deconvolution artifacts need to be carefully reviewed (see section "FAQ: Deconvolution artifacts"), and over-processing needs to be avoided in most cases. It is also advisable to keep the raw data for future processing and comparison.

Can I deconvolve transmitted light brightfield images?

Generally, deconvolution cannot process brightfield data for the following two reasons: 1) PSF would be wrong as it does not include the condenser; 2) Brightfield signals originate from light absorption, which is a nonlinear process and mathematically non-tractable.

However, there is one generally accepted linear approximation possible under the following conditions: 1) The sample is approximately non-absorbent or at least very thin so that absorption can be neglected; 2) The image needs to be gray-level inverted, then deconvolved as a fluorescent image (the image can be inverted once again afterward); 3) The brightfield system must be good enough Köhlered, so the PSF becomes close to that of a fluorescent system.

FAQ: Deconvolution artifacts

To confidently use deconvolution first requires an understanding of what can potentially go wrong. This section covers the origins and appearance the most common deconvolution artifacts, as well as how to avoid them.

Where do deconvolution artifacts come from?

1. Erroneous raw data

   Many mishaps can happen during image acquisition. From the instrument side, optical misalignment, light source flickering (mercury lamps, metal halide lamps, lasers), and detector artifact (camera dead pixel or electromagnetic interference of PMT) impact image quality. From the sample side, photobleaching during z-stack acquisition, using of non-standard cover glass, sample movement, and high background signal (resulting for example from tissue autofluorescence, fluorescent signals in cell culture medium or immersion medium, or environmental stray light) also can influence quality. And from the imaging side, incorrectly recorded metadata (e.g., objective NA or emission wavelength), poor lateral/axial sampling, and detector over-saturation can skew the data collected.

2. Incorrect deconvolution settings

   PSF setting is critical to deconvolution performance, especially for the iterative-based algorithms where the same PSF is repeatedly applied. Incorrect PSF settings lead to strong artifacts and for theoretical PSF, the wrong metadata input. Most software assumes the same refractive indices between embedding and immersion media, thus you need to change them manually when, for example, using oil objectives on a water embedded sample when working with the theoretical PSF.

   For measured PSF, you will need to use a PSF acquired with the imaging conditions matching your sample's condition (objectives, wavelength, refractive indices of embedding and immersion mediums, and pinhole size). The parameter regularization deals with noise. Generally, the higher the noise level, the higher the order of regularization is required.

3. Overprocessing

   Overprocessing is common in deconvolution, particularly when maximum resolution improvement is the goal. It usually happens when a very high restoration "strength" has been selected, or too many iterations have occurred while using an iterative-based method, or both. Raw data with low dynamic range and poor SNR is more likely to have overprocessing artifacts.

What do deconvolution artifacts look like?

1. Disappearing or inaccurate structures

   It is common to lose delicate and dim structures after deconvolution processing. This is most likely caused by the noise reduction of the regularization filter or excessive use of the smoothing filter. Using measured PSF with a high level of noise also can lead to the disappearance of small structures. On the other hand, deconvolution can enlarge and expand very bright structures beyond their physical size, especially if the pixels are saturated. Additional patterns can also be generated in the background for raw data with poor dynamic range and high background noise, especially when using the inverse filter-based method. See Figure 17 for examples of a few deconvolution artifacts.

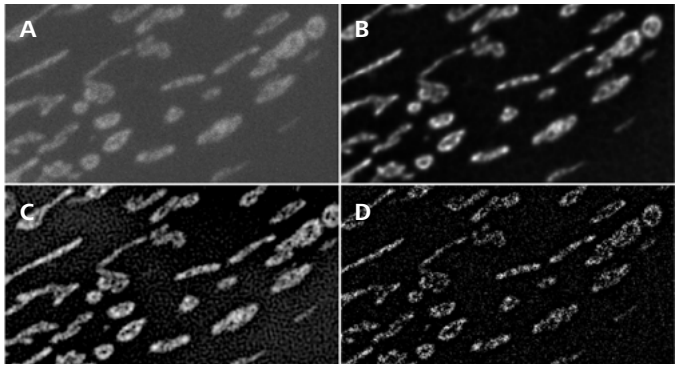

Figure 17 *Example of deconvolution artifacts. A) raw data of mitochondria structures acquired using a widefield fluorescent microscope. B) a good deconvolution example using the constrained iterative method. C) a poor deconvolution example showing invention of structures in the background. D) a poor deconvolution example showing enhanced salt-and-pepper noise and disappearance of structures.*

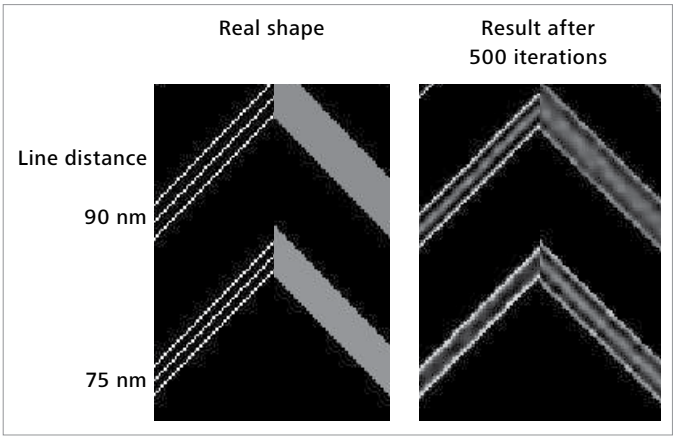

Figure 18 *Simulated objects mimicking single lines or one solid line. Lines can appear and disappear when too many iterations are applied for deconvolution.*

2. Axial distortion

   Axial distortion is usually formed by strong spherical aberration and is not a deconvolution artifact. It should be visible in the raw data but is more prominent after deconvolution since the SNR and contrast are improved. Axial distortion can be corrected using an advanced depth variance algorithm. See Figure 3 for details.

3. Salt-and-pepper noise

   Remnant salt-and-pepper noise can still be visible after deconvolution when the regularization filter is too low.

4. Sheets/stripes pattern above and below samples

   Deconvolution might enhance a horizontal or vertical line pattern that was caused by a camera dead pixel or an extremely bright structure residing near the acquired volume. Strong spherical aberration of raw data or use of a wrong measured PSF could lead to a sheet of light above and below the sample. See Figure 3 for an example.

5. Ringing artifact

   Ringing artifact is the appearance of one or multiple ripple patterns around bright structures in the deconvolved image. It happens mostly with neighbor-based or inverse filter-based methods. Change to an iterative-based method should resolve it.

How to avoid or compensate for deconvolution artifacts?

1. Examine the raw data

   By carefully adjusting the brightness and contrast of the raw image and displaying the 3D data set in an orthogonal view (view of XY, XZ and YZ projections simultaneously, see Figure 2), many imaging problems, such as spherical aberration or photobleaching can be identified. Such information will guide us for the proper settings or corrections.

2. Start with default deconvolution parameter

   Most commercial deconvolution software, such as ZEN Deconvolution, has a smart default setting. Depending on the input image type, which is obtained from the image's metadata, the software will automatically assign a set of suitable parameters, including the algorithm, restoration strength (determined automatically with the help of Generalized Cross Validation method), regularization, number of iterations, and more. It's safe to start with such default settings.

3. Compare the raw data with the deconvolved image

   Deconvolution can improve resolution and SNR, but it should not create, change, or remove existing structures in the raw image. It is always advised to keep the raw data and compare the deconvolved and raw images in a synchronized view, such as the split view function in ZEN.

4. Compare different deconvolution algorithms or settings

   When a suspected deconvolution artifact is not visually present in the raw data, try a different deconvolution algorithm, like switching from a constrained iterative method to a regularized inverse filter method. Different algorithms may have a different impact on a particular structure or background. A careful comparison of the data might reveal the artifact. Additionally, reducing the restoration strength or the number of iterations also can lead to fewer artifacts.

5. Activate image correction when available

   Some imaging artifacts, such as photobleaching, dead camera pixel, lamp flicker, fluorescence background, and spherical aberration can be mathematically compensated in the deconvolution program. Activate one or multiple such corrections when imaging artifacts are identified within the raw data.

Closing remarks

Deconvolution has become an important asset for almost any microscope imaging modality, be it camera or point detector based. However, the phrase "garbage in, garbage out" can be applied to DCV, so you must make sure that your raw data are of a sufficient quality before starting. Then, the question of whether iterative algorithms will produce quantitative results can be answered "yes" with a good conscience. In addition, DCV will not only play its strength in removing blur and increasing the SNR, but also provide a significant increase in resolution. As algorithms continue to be refined and constraints are better matched to the sample structures, we can expect DCV to play an ever-increasing role in image processing.

Bibliography

- Biggs, D.S.C.: Accelerated iterative Blind Deconvolution. Ph.D. Thesis, University of Auckland, New Zealand (1996)
- Born, Max & Wolf, Emil: Principles of Optics, Pergamon Press (1959)
- van Cittert, P. H.: "Zum Einfluß der Spaltbreite auf die Intensitätsverteilung in Spektrallinien. II," Z. Phys. 69, 298–308 (1931)
- Gibson, S.F. & Lanni, F.: Experimental test of an analytical model of aberration in an oil-immersion objective lens used in three-dimensional light microscopy, JOSAA, Vol 9, Issue 1 (1992)
- [SIM_02] M. G. L. Gustafsson, J. Microsc. 2000, 198, 82.
- Holmes T.J., Biggs D., Abu-Tarif A.: Blind Deconvolution. In: Pawley J. (eds) Handbook Of Biological Confocal Microscopy. Springer, Boston, MA. https://doi.org/10.1007/978-0-387-45524-2_24 (2006)
- [SIM_04] X. Huang, J. Fan, L. Li, H. Liu, R. Wu, Y. Wu, L. Wie, H. Mao, A. Lal, P. Xie, L. Tang, Y. Z., Y. Liu, S. Tan, L. Chen, Nat. Biotechnol. 2018, 36, 451.
- Jansson, P. A. ed.: Deconvolution of Images and Spectra (2Nd Ed.) (Academic Press, Inc., Orlando, FL, USA (1996)
- [SIM_01] A. Löschberger, Y. Novikau, R. Netz, M.-C. Spindler, R. Benavente, T. Klein, M. Sauer, I. Kleppe, "Super-resolution imaging by dual iterative structured illumination microscopy", Carl Zeiss Microscopy GmbH, April 2021
- Lucy, L.B.: An iterative technique for the rectification of observed distributions, Astron. J., 1974, 79:745-754
- Meinel, Edward S.: Origins of linear and nonlinear recursive restoration algorithms, J. Opt. Soc. Am. A 3, 787-799 (1986)
- Richardson W.H., Bayesian-based iterative method for image restoration. J. Opt. Soc. Am., 1972, 62 (6): 55-59
- Roth S. et. al.: Optical Photon Reassignment Microscopy (OPRA) (2013), arXiv:1306.6230
- Schaefer LH, Schuster D, Herz H.: Generalized approach for accelerated maximum likelihood-based image restoration applied to three-dimensional fluorescence microscopy. J Microsc. 2001 Nov;204(Pt 2):99-107. doi: 10.1046/j.1365-2818.2001.00949.x. PMID: 11737543.
- Schaefer et. al. "Structured illumination microscopy: artefact analysis and reduction utilizing a parameter optimization approach" Journal of Microscopy, Vol. 216, Pt 2 November 2004, pp. 165–174
- Schaefer, Lutz & Schuster, D.: Structured illumination microscopy: improved spatial resolution using regularized inverse filtering (2006)
- Sheppard C.J.R.: Super-resolution in confocal imaging, Optik - International Journal for Light and Electron Optics 80(2):53 (1988)
- Sheppard C.J.R.: The Development of Microscopy for Super-Resolution: Confocal Microscopy, and Image Scanning Microscopy (2021), Applied Sciences 11(19):8981
- [SIM_03] Dr. Jörg Siebenmorgen, Dr. Yauheni Novikau, Ralf Wolleschensky, Dr. Klaus Weisshart, Dr. Ingo Kleppe, "Introducing Lattice SIM for ZEISS Elyra 7 Structured Illumination Microscopy with a 3D Lattice for Live Cell Imaging", December 2018
- Tikhonov, A.N. & Arsenin, V.Y.: Solutions of ill Posed Problems. Wiley, New York (1977)
- Van der Voort, H.T.M. and Strasters, K.C.: Restoration of confocal images for quantitative analysis. J. Micros., 178, 165-181 (1977)
- Verveer, Peter J. and Jovin, Thomas M.: Efficient superresolution restoration algorithms using maximum a posteriori estimations with application to fluorescence microscopy J. Opt. Soc. Am. A,14, 1696-1706 (1997)
- Wallace, W. et al.: A workingperson's guide to deconvolution, Biotechniques, Nov. 2001, Vol 31, No 5
- Wiener, Norbert: Extrapolation, Interpolation, and Smoothing of Stationary Time Series. Wiley, New York NY (1949)
- [SIM_05] Y. Zhang, S. Lang, H. Wang, J. Liao, Y. Gong, J. Opt. Soc. Am. A 2019, 36, 173

Carl Zeiss Microscopy GmbH
07745 Jena, Germany
microscopy@zeiss.com
www.zeiss.com/microscopy